J. Membrane Biol. 15, 277–318 (1974)

Discrimination of Monovalent Inorganic Cations by "Tight" Junctions of Gallbladder Epithelium

Julio H. Moreno and Jared M. Diamond

Physiology Department, University of California Medical Center, Los Angeles, California 90024

Received 14 June 1973; revised 18 October 1973

Summary. Relative permeability coefficients (*P*'s) for Li^+, Na^+, K^+, Rb^+, Cs^+, NH_4^+ and Tl^+ have been measured in gallbladders of several animal species. Small differences are observed among individual animals of the same species in the *P* values for a given ion. Individual variations in *P* values of different ions are closely correlated, permitting construction of so-called selectivity isotherms. Exposure to pH 4 reversibly shifts *P* values along the same isotherms as those defined by individual variation. Changes in partial conductances with pH indicate that cation conductance is controlled by acidic sites with an apparent pK_a value near 4.5, anion conductance by basic sites with an apparent pK_a value below 3. Isotherms for rabbit gallbladder and bullfrog gallbladder are quite similar, and the small differences between them are probably attributable to a narrower permeation channel in rabbit than in bullfrog. Permeability ratios for eight other epithelia with leaky "tight junctions" fall close to the isotherms for rabbit and bullfrog gallbladders. The observed isotherms, sequences, and pH-dependence of alkali cation permeability are strikingly consistent with Eisenman's interpretation that selectivity is controlled by site field strength. Variation in P_{Tl} and P_{NH_4} is also correlated with variation in site field strength. Comparison with isotherms or "selectivity fingerprints" for glass electrodes and macrocyclic carriers suggests that the permeation channel in gallbladder tight junctions is highly hydrated; and that sites in the gallbladder may possess net charge and may not be in a precisely regular spatial array.

Discrimination of the two naturally occurring alkali cations, K^+ and Na^+, presents one of the major interpretative problems in membrane biology. In most biological membranes there are large differences between the permeabilities not only of these two cations but also of the other three alkali cations, Li^+, Cs^+ and Rb^+. An essential clue to the mechanism of this discrimination is that only certain ones of the 120 possible permutations of the five alkali cations ($5! = 120$) have been observed as biological permeability sequences (Eisenman, 1961, 1962, 1965*a*). Furthermore, there are quantitative regularities in cation discrimination: only certain ranges of permeability ratios are associated with each of the commonly occurring

permeability sequences. These quantitative regularities are conveniently summarized by so-called empirical selectivity isotherms, in which the relative permeability of each cation in turn is plotted as a function of the permeability ratio for one pair of cations measured in the same system (Eisenman, 1961, 1962, 1965*a*). Nonliving membranes such as glass electrodes are found to exhibit essentially the same alkali cation permeability sequences as seen in biological systems, and selectivity isotherms for nonliving and biological systems are similar. Eisenman showed that the observed selectivity sequences could be correctly predicted by computing for each cation the difference between its hydration energy and its Coulomb interaction energy with membrane negative sites, as a function of the site's electrostatic field strength. The implication of Eisenman's analysis is that cation discrimination can be interpreted mainly in terms of differences in the free energy of cation transfer at equilibrium between water and membrane sites; and that biological membranes which exhibit different permeability sequences do so as a result of possessing anionic sites of different effective field strength (Eisenman, 1961, 1962, 1965*a*; Diamond & Wright, 1969).

Recently, it has been recognized that there are detailed differences between sets of selectivity isotherms in different physical systems, associated with differences in molecular structure of the sites and hence in ion-site forces (Eisenman, Szabo, Ciani, McLaughlin & Krasne, 1973; Krasne & Eisenman, 1973). Similar second-order differences are beginning to be recognized among biological systems. Such details of selectivity isotherms are of much interest, because they may serve as a "fingerprint" permitting identification of the type of site present in a membrane of unknown structure.

The first aim of the present study was to construct selectivity isotherms for transepithelial permeation of alkali cations in gallbladder. The cation permeation pathway in gallbladder is located in the so-named "tight" junctions between cells (Barry, Diamond & Wright, 1971; Frömter, 1972; Frömter & Diamond, 1972). Our hope was that, by confining attention to a single preparation in various states, we might be measuring sets of permeability ratios whose variation between experiments was due primarily to variation in a single physical variable. Comparison of diverse biological membranes is more likely to introduce scatter into selectivity isotherms, since the membranes might differ in degree of hydration, type of permeation mechanism, and molecular class of site as well as in field strength. In practice, we found that there are consistent patterns of variation in relative permeability coefficients among gallbladders belonging to different animal species, to different individuals of the same species, and to the same individual but at different pH's. This variation has been utilized to construct selectivity

isotherms in gallbladder, for comparison with isotherms in well-understood physical systems such as glass electrodes and macrocyclic carriers.

The second aim was to construct isotherms for two additional monovalent cations whose interactions with anionic sites are unlikely to be well represented by a model assuming a monopolar ion and predominantly monopolar coulombic forces, in contrast to the simple behavior of the alkali cations. Ion polarization and covalent interactions might be important for thallium (Tl^+), while the spatial configuration of the site might be important for NH_4^+ because of its multipolar charge distribution. Thus, it is *a priori* unclear whether the variations in site field strength that largely control alkali cation discrimination would also be important in Tl^+ and NH_4^+ selectivity, or whether other factors specific to Tl^+ or NH_4^+ would be more important. In addition, the very existence of these specific factors means that Tl^+ and NH_4^+ isotherms might prove particularly sensitive probes of site structure. Some of these results have been reported in preliminary form (Moreno & Diamond, 1973*a*, *b*).

Materials and Methods

Dissection and Mounting

Experimental material consisted of gallbladders from bullfrogs (*Rana catesbiana*) weighing ca. 350 g, from white rabbits weighing 2.5 to 3 kg, from goldfish (*Carassius auratus*) weighing ca. 200 g, and from guinea-pigs weighing 300 to 500 g. Techniques for obtaining an *in vitro* preparation of gallbladder and measuring transepithelial potential differences (abbreviated p.d.'s) were generally similar to those described previously (Barry & Diamond, 1970), the main differences being that our solutions contained K^+ and phosphate (*see* next two paragraphs) and that gallbladders were mounted between chambers rather than studied as sacs. Briefly, the gallbladder was removed from the animal, carefully rinsed free of bile, cut open, and mounted as a flat sheet between two Lucite half-chambers with a window area of 10 mm^2. Each chamber contained 10 ml of solution, which was vigorously stirred by a magnetic stirring bar. As estimated from the half time of NaCl dilution potentials (Diamond, 1966), the average unstirred layer thickness at the mucosal face of the tissue was 95 μ in frog, 118 μ in rabbit, 128 μ in goldfish, and 104 μ in guinea-pig. As discussed previously by Wright, Barry and Diamond (1971), "edge conductance" associated with tissue damaged at the border by the chambers is negligible, since tissue conductance per cm^2 is independent of the window area. However, we found that tissue deterioration, as judged by NaCl dilution potentials, was more rapid with a window area of 79 mm^2 than 30 or 10 mm^2, hence 10-mm^2 windows were used.

Solutions

The standard bathing solution had the following composition (mM=millimolal): 150 mM NaCl, 0.25 mM $CaCl_2$, 2.31 mM K_2HPO_4, 0.38 mM KH_2PO_4, pH 7.4. Biionic potentials were measured by replacing 150 mM NaCl with 150 mM KCl, LiCl, RbCl,

CsCl, or NH_4Cl. Dilution potentials were measured by reducing NaCl concentration to 75 mM by isosmotic replacement with mannitol. Solutions at pH 9.5, 6.0, 5.8 and 5.7 were identical except that the K_2HPO_4/KH_2PO_4 ratio was altered to yield the desired pH, maintaining (K^+) constant at 5 mM. In solutions at pH 5.0, 4.1 and 3.8 the K_2HPO_4/KH_2PO_4 buffer was replaced by a 5-mM K^+ phthalate buffer. In solutions at pH 3.0, 2.7 and 2.5 the buffer was a KH_2PO_4/H_3PO_4 mixture also containing 5 mM K^+. Since the solubility of TlCl is low, experiments involving Tl^+ were carried out in solutions in which all Cl^- was replaced by NO_3^- but composition was otherwise as described above.

In contrast to the results of previous studies (e.g., Diamond & Harrison, 1966; Wright & Diamond, 1968, 1969), Wright *et al.* (1971) and Barry *et al.* (1971) found that the electrical properties of rabbit gallbladder were time-dependent: with time after dissection, conductance increased, and permeability ratios shifted towards free-solution mobility ratios. These changes were largely consistent with those expected from gradual development of a free-solution shunt. The procedure used by Wright *et al.* (1971) and Barry *et al.* (1971) differed from procedures used in previous studies in that the bathing solutions contained neither phosphate (TRIS or HEPES being instead used as buffers) nor K^+. Experiments we carried out to examine the effect of bathing solution composition on the electrical properties of gallbladder make it clear that the absence of K^+ and of phosphate was the reason for the progressive development of a shunt in the studies of Wright *et al.* (1971) and Barry *et al.* (1971). In eight experiments in rabbit gallbladder we found that either replacement of phosphate by TRIS or HEPES, or removal of K^+ from our standard bathing solution, caused the NaCl dilution potential progressively to decrease towards the free-solution junction potential, and that over short times this effect was reversible. 3 mM K^+ was as effective as 5 mM K^+ at preventing this deterioration, and Cs^+ as well as K^+ prevented deterioration. Wiedner and Wright (*personal communication*) similarly observed that a shunt does not develop in the presence of K^+ phosphate. In our experiments using 5 mM K^+, 2.7 mM phosphate, and chambers of 10 mm^2 area, we found that gallbladder permselectivity, as measured by conductance and dilution potentials, remained intact for long times. On the average, in frog gallbladder over the first two hours after mounting, the conductance *decreased* by 19%, and the calculated permeability ratio P_{Na}/P_{Cl} *increased* (away from the free-solution mobility ratio) from 3.7 to 6.1, indicating that a shunt was closing rather than opening with time. In rabbit gallbladder over the first 2 hr, conductance on the average increased by 8%, and P_{Na}/P_{Cl} increased from 7.0 to 7.5. Thus, tissue deterioration as expressed in progressive development of a free-solution shunt was successfully minimized.

Electrical Measurements

Transepithelial p.d.'s were recorded on a Keithley 610B electrometer connected to a Rickadenki Kogyo three-channel recorder. The electrodes used with chloride solutions were pairs of Ag/AgCl electrodes prepared so that the difference in potential with both electrodes in the same 150-mM Cl^- solution was stable and less than 0.1 mV. All transepithelial p.d.'s measured with asymmetrical bathing solutions were corrected for the difference in electrode potentials, $E=(RT/F)\ln(a'_{Cl}/a''_{Cl})$, where a'_{Cl}/a''_{Cl} is the chloride activity ratio as estimated from activity coefficients in Robinson and Stokes (1970). The electrodes used with nitrate solutions were calomel electrodes connected to the bathing solutions by bridges of 150 mM $NaNO_3$ Ringer's solution immobilized by 4% agar. Transepithelial p.d.'s were corrected for the junction potential, calculated as described by Barry and Diamond (1970).

Transepithelial conductance in symmetrical 150 mM NaCl or $NaNO_3$ Ringer's solutions was measured at least every 15 min, by noting the p.d. change resulting from

a 10-μA direct current pulse applied for 4 sec. The current was delivered by a pair of Ag/AgCl electrodes connected to opposite sides of the gallbladder by bridges composed of 150 mM NaCl or 150 mM $NaNO_3$ Ringer's solution in 4% agar (depending on the bathing solution used), the bridge tips being 3.5 cm from the tissue. Current polarity was changed after each pulse. Voltage was recorded by a pair of Ag/AgCl electrodes or $NaNO_3$-agar bridges (depending on the bathing solution used) whose tips were less than 3 mm from the tissue, and all conductance values were corrected for the saline resistance measured with the electrodes in the same position but the tissue removed. With the current pulses used, the error introduced into resistance determinations by the transport-number effect (Barry & Hope, 1969*a*, *b*; Wedner & Diamond, 1969) was negligible.

Extraction of Permeability Ratios

We extracted permeability ratios from measured p.d.'s by means of the Goldman-Hodgkin-Katz equation, corrected as follows for the presence of a shunt.[1] For two cations, M^+ and N^+, and one anion, X^-, the Goldman-Hodgkin-Katz equation reads

$$\Delta E = E' - E'' = \frac{-RT}{F} \ln \frac{P_M \gamma'_M [M]' + P_N \gamma'_N [N]' + P_X \gamma''_X [X]''}{P_M \gamma''_M [M]'' + P_N \gamma''_N [N]'' + P_X \gamma'_X [X]'} \tag{1}$$

where superscripts $''$ and $'$ refer to the two bathing solutions, E is voltage, R, T and F have their usual meanings, P's are relative permeability coefficients, γ's activity coefficients (from Robinson & Stokes, 1970), and brackets represent concentrations. The total partial conductance of the ionic species i, $G_i(t)$, consists in general of the sum of its conductance in native membrane, $G_i(m)$, plus its conductance in the shunt, $G_i(s)$. That is,

$$G_i(t) = G_i(m) + G_i(s). \tag{2}$$

1 The numerical values of ion permeability ratios calculated from diffusion potential measurements may depend upon what permeation mechanism one assumes and hence upon what equation one uses. Barry *et al.* (1971) and Machen and Diamond (1972) showed that both at neutral pH and at low pH the electrical properties of rabbit gallbladder are well described by the model of a thick membrane with fixed neutral sites and a parallel shunt (Barry & Diamond, 1971). This model is also expected to describe frog gallbladder, whose salient electrical properties resemble those of rabbit gallbladder. [For example, Bindslev and Wright (*personal communication*) found a linear conductance-concentration relation and linear instantaneous current-voltage relation, and our unpublished observations show that P_{Na}/P_{Cl} is approximately independent of ionic strength up to 0.5 M NaCl.] A practical problem arises, in that the equation derived from this model for biionic potentials [Barry & Diamond, 1971, Eq. (62)] is too complex to use for calculations. However, Barry *et al.* (1971) and Machen and Diamond (1972) showed that the thick-membrane and the thin-membrane fixed-neutral-site-plus-shunt equations yield virtually the same permeability ratios for dilution potentials, although the two equations are formally distinct; the same finding was true for the thick- and the thin-membrane equations without shunt, both for dilution potentials and biionic potentials; and the thin-membrane equation without shunt is formally identical to the well-known Goldman-Hodgkin-Katz equation or constant-field equation (Barry & Diamond, 1971). It can be shown that our procedure described in Eqs. (1)–(7) is formally identical to using the thin-fixed-neutral-site-plus-shunt equation [Barry & Diamond, 1971, Eq. (114)], generalized to mixed cation solutions and assuming that the nonideal activity factor n (Barry & Diamond, 1971, p. 298; Barry *et al.*, 1971, pp. 383–388) equals 1.0 for each pair of cations studied.

As discussed by Barry *et al.* (1971) and further supported by studies on the permeation of organic cations (Moreno & Diamond, 1974*a*), the low anion conductance of the gallbladder may be assumed to be entirely in a shunt in which ion mobilities have the same ratios as do the free-solution mobilities u_i. That is,

$$G_X(m)=0, \quad G_X(t)=G_X(s) \tag{3}$$

and

$$G_M(s)/G_X(s)=u_M/u_X, \quad G_N(s)/G_X(s)=u_N/u_X. \tag{4}$$

Therefore, an apparent cation-to-anion permeability ratio $P_M(\text{app})/P_X(\text{app})$, obtained by inserting the measured ΔE into Eq. (1), actually represents

$$\frac{P_M(\text{app})}{P_X(\text{app})}=\frac{G_M(t)}{G_X(t)}=\frac{G_M(m)+G_M(s)}{G_X(s)}=\frac{G_M(m)}{G_X(s)}+\frac{u_M}{u_X}. \tag{5}$$

An equation analogous to Eq. (5) may be written for the other cation, N. The cation-to-cation permeability ratio for native membrane, $P_M(m)/P_N(m)$, corrected for cation conductance in the shunt, is defined by

$$P_M(m)/P_N(m)\equiv G_M(m)/G_N(m). \tag{6}$$

Combination of Eq. (6) with Eq. (5) written for each cation yields

$$\frac{P_M(m)}{P_N(m)}=\left(\frac{P_M(\text{app})}{P_X(\text{app})}-\frac{u_M}{u_X}\right)\Big/\left(\frac{P_N(\text{app})}{P_X(\text{app})}-\frac{u_N}{u_X}\right). \tag{7}$$

In practice, $P_{Na}(\text{app})/P_{Cl}(\text{app})$ was calculated by inserting a measured dilution potential into Eq. (1); $P_M(\text{app})/P_{Cl}(\text{app})$, where M represents any other cation, was calculated by inserting the measured Na:M biionic potential and the calculated $P_{Na}(\text{app})/P_{Cl}(\text{app})$ into Eq. (1); and $P_M(m)/P_{Na}(m)$ was then calculated from Eq. (7). In the Results and Discussion sections of this paper, these corrected ratios $P_M(m)/P_{Na}(m)$ will be referred to simply as P_M/P_{Na}.

Mobility ratios were calculated from transport-number ratios at 150 mM for LiCl, NaCl, KCl, and NH_4Cl (MacInnes, 1961). For $TlNO_3$, $NaNO_3$, CsCl and RbCl the transport numbers at physiological concentrations were unavailable, hence the mobility ratio was taken as the ratio of limiting equivalent conductances (Harned & Owen, 1957). The error introduced by this approximation should be small, since the transport-number ratio at 150 mM and the limiting equivalent conductance ratio differ by only 2.9% for LiCl, 1.8% for NaCl, 0.1% for KCl, and 0.0% for NH_4Cl. The mobility ratios calculated in these ways were $u_{Na}/u_{Cl}=0.623$, $u_K/u_{Cl}=0.956$, $u_{NH_4}/u_{Cl}=0.965$, $u_{Li}/u_{Cl}=0.457$, $u_{Cs}/u_{Cl}=1.012$, $u_{Rb}/u_{Cl}=1.012$, $u_{Na}/u_{NO_3}=0.701$, $u_{Tl}/u_{NO_3}=1.04$.

As discussed in the section on solutions, shunt conductance was much lower in our experiments than in the experiments of Barry *et al.* (1971), and the shunt correction accordingly made less difference in calculated permeability ratios, especially for the more permeant ions. For example, in frog gallbladder the shunt correction left P_K/P_{Rb} unaffected until the fourth decimal place. The largest effect was on P_K/P_{Cs} in rabbit gallbladder, where the shunt correction increased $P_K(\text{app})/P_{Cs}(\text{app})=2.81$ to $P_K(m)/P_{Cs}(m)=3.33$.

Calculations were carried out on an IBM 360 computer, using APL language. Errors are expressed as standard errors of the mean.

Experimental Protocol

All experiments were performed at 23 °C. The serosal solution was always 150 mM NaCl or 150 mM $NaNO_3$ Ringer's solution at the same pH as the mucosal solution,

and was renewed at least every 10 min. For conductance measurements a mucosal solution identical in composition to the serosal solution was used. The p.d. in the absence of ion concentration gradients was small or negligible (average $\pm$SEM at the start of the experiment, 2.8 ± 0.2 mV (n=16) in frog gallbladder, 0.5 ± 0.2 mV (n=12) in rabbit gallbladder, serosal solution positive to mucosa, in NaCl Ringer's solution at pH 7.4). Dilution potentials were measured by reducing (NaCl) or ($NaNO_3$) in the mucosal solution to 75 mM by isosmotic replacement with mannitol; biionic potentials, by replacing all NaCl or $NaNO_3$ of the mucosal solution mole-for-mole by the Cl^- or NO_3^- salt of another cation. After each two measurements of biionic potentials, a 2:1 NaCl dilution potential was measured. A set of measurements at pH values other than 7.4 was always "bracketed" by a preceding and a subsequent set at pH 7.4, to be certain that effects of pH were reversible.

The p.d. values used for calculating all permeability ratios reported in this paper were steady-state or quasi-steady-state values, achieved generally within a fraction of a minute after a change of solutions and maintained for at least many minutes thereafter. The form of the transient p.d. change during the early seconds after a change of solutions depends upon three effects: equilibration of ion concentrations at the mucosal face of the gallbladder, by diffusion through adjacent unstirred layers; transient appearance and subsequent disappearance of a junction potential between the new bathing solution and an unstirred layer of old bathing solution adjacent to the gallbladder; and effects attributable to a low-resistance series resistor in the gallbladder. Details of these transients, and illustrations of their forms (Figs. 15–17), are presented in the Appendix to this paper.

Results

Types of Variation in Permeability Ratios

The construction of selectivity isotherms for gallbladder will utilize three consistent sources of variation in steady-state permeability ratios: variation arising from differences between individual animals, from differences between species, and from differences in pH. These three factors produce variation in the relative permeability coefficient of every cation. The fact that there are good correlations between the variation in any one cation and the variation in any other cation is what makes construction of selectivity isotherms meaningful and possible. Each type of variation will be illustrated by describing it in detail for the cation trio NH_4^+, Na^+ and K^+. The entirely analogous results for all cations together will then be summarized more briefly in Fig. 7.

Individual Variation. K^+:Na^+ and NH_4^+:Na^+ biionic potentials were compared at pH 7.4 in gallbladders from 20 frogs. P_{Na}/P_K ranged from 0.41 to 0.81, P_{NH_4}/P_K from 0.69 to 1.42, and P_{NH_4}/P_{Na} from 1.56 to 1.90. As illustrated in Fig. 1, variations in these ratios were closely correlated: the higher the value of P_{Na}/P_K in an individual frog, the higher also the value of P_{NH_4}/P_K. Since each permeability ratio could be either greater or less than the corresponding free-solution mobility ratio ($u_{Na}/u_K = 0.652$, $u_{NH_4}/u_K = 1.008$), this

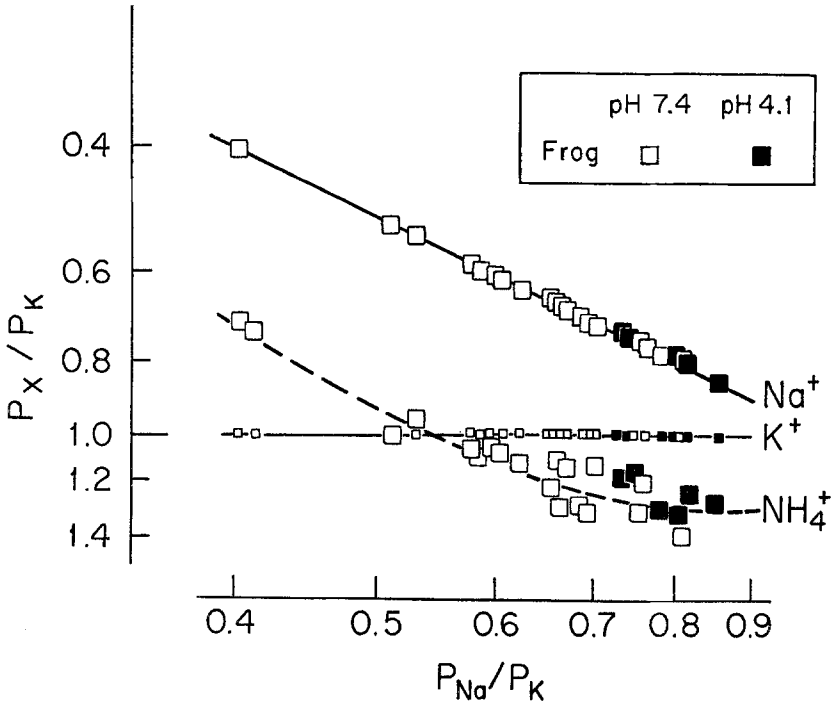

Fig. 1. NH_4^+, Na^+ and K^+ isotherms in frog gallbladder. The abscissa gives P_{Na}/P_K values measured in the gallbladders of each of 20 individual frogs, while the ordinate gives P_X/P_K values in the same gallbladder, where X may be either NH_4^+, Na^+ or K^+. The scales are logarithmic. Thus, sets of three points located along the same imaginary vertical line represent relative permeability coefficients for the three ions in a single animal. The K^+ points automatically fall along the horizontal line $P_X/P_K = 1.0$, and the Na^+ points automatically fall along the line of identity. Note that the NH_4^+ points cluster closely about the second-order polynomial fitted through them by least-mean-squares, the NH_4^+ isotherm. That this is the case, rather than that the NH_4^+ points scatter at random, means that P_{NH_4}/P_K and P_{Na}/P_K are closely correlated (e.g., because both are determined by the same physical variable). Points □ and ■ were measured at pH 7.4 and 4.1, respectively. Points for K^+ are drawn smaller, to prevent confusion with points for NH_4^+

variation could not be due to varying shunt conductance (all P values are corrected for the shunt) or an inadequate shunt correction. Fig. 7 will demonstrate correlated trends for all other cations studied in frog gallbladder.

Fig. 2 demonstrates the existence of qualitatively identical individual variation among gallbladders from rabbits. P_{Na}/P_K ranged from 0.29 to 0.56, P_{NH_4}/P_K from 0.43 to 0.81, and P_{NH_4}/P_{Na} from 1.32 to 1.65. Rabbits with higher values of P_{Na}/P_K also have higher values of P_{NH_4}/P_K. Fig. 7 will demonstrate correlated trends for the other cations in rabbit gallbladder.

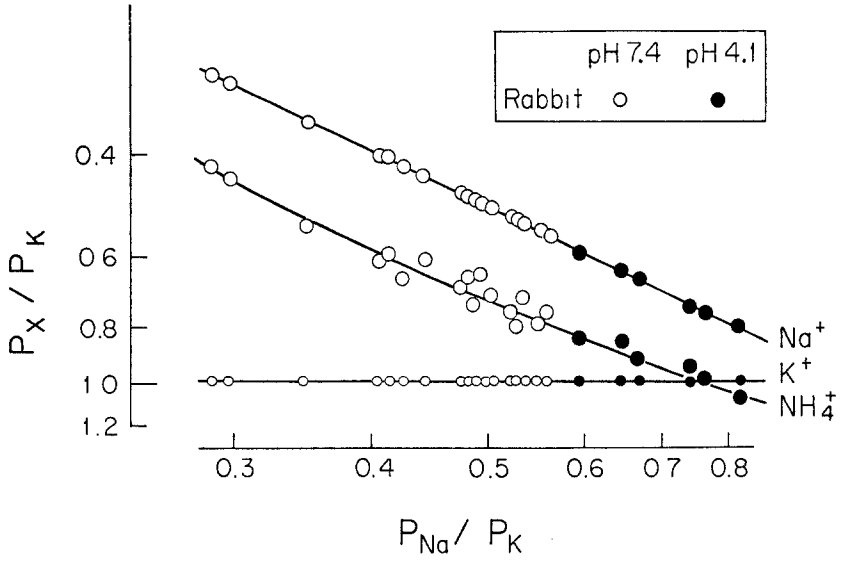

Fig. 2. NH_4^+, Na^+ and K^+ isotherms in rabbit gallbladder, constructed in the same manner as Fig. 1. ○ and ●, measurements at pH 7.4 and 4.1, respectively. Points for K^+ are drawn smaller

Species Variation. P_{Na}/P_K and P_{NH_4}/P_K were measured in gallbladders from two guinea-pigs and one goldfish in addition to the above-mentioned frogs and rabbits. For guinea-pig, rabbit, frog and goldfish, average values of P_{Na}/P_K were, respectively, 0.34, 0.62, 0.70 and 0.83; of P_{NH_4}/P_K, 0.43, 0.85, 1.16 and 1.15. Thus, species variation in these ratios was also correlated: species with a higher P_{Na}/P_K also had a higher P_{NH_4}/P_K.

Fig. 3, which combines measurements on all individuals of all four species, shows that individual variation and species variation define approximately the same isotherms. In their P_{NH_4}/P_K and P_{Na}/P_K ratios, guinea-pigs are similar to three individual rabbits with the lowest values of these ratios. Goldfish is similar to the individual frog with the highest values of these ratios. The individual frogs with the lower values of these ratios are similar to the individual rabbits with higher values. Thus, it appears that differences among species mainly involve the same kind of variation as, and are merely a quantitative extension of, differences among individuals of the same species. Closer examination shows that this agreement is not perfect: for a given value of P_{Na}/P_K, P_{NH_4}/P_K is always slightly higher in frog than in rabbit. Fig. 7 will display similar approximate agreement for the other cations, and the significance of the second-order deviations from this agreement will be discussed on pp. 296–299.

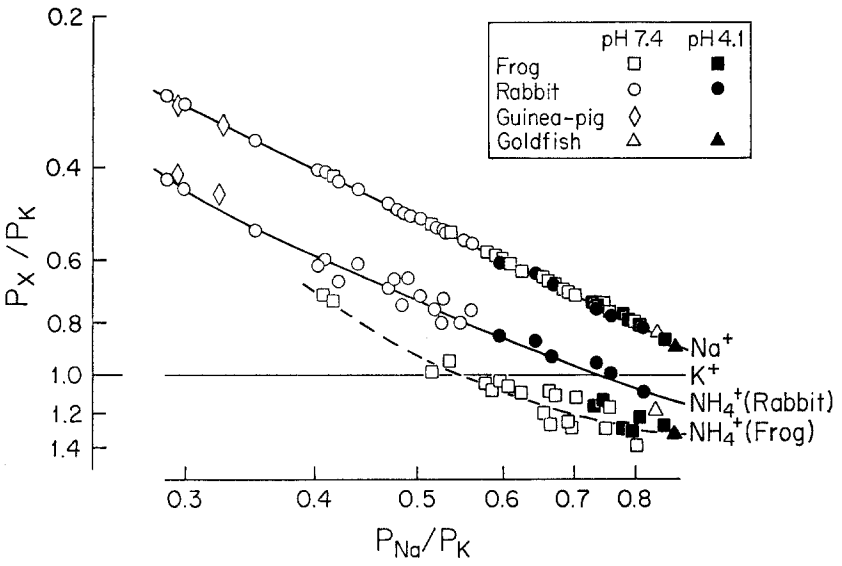

Fig. 3. Combined NH_4^+, Na^+ and K^+ isotherms for gallbladders of four species, constructed in Fig. 1. Each set of points located along a vertical line is based on one animal. Open symbols and closed symbols represent measurements at pH 7.4 and 4.1, respectively: ○ and ●, rabbit; □ and ■, frog; ◇, guinea-pig; △ and ▲, goldfish. Points for K^+ all fall along the horizontal line $P_X/P_K = 1.0$ and are omitted for clarity. Note that the NH_4^+ points in frog and those in rabbit each cluster about the second-order polynomial fitted through them by least-mean-squares, the NH_4^+ isotherm for that species. Note also that the NH_4^+ isotherms for frog and for rabbit are close but not coincident

pH Variation. Wright and Diamond (1968) showed that NaCl or KCl dilution potentials in rabbit gallbladder reversed sign below about pH 3, and that P_{Cs}/P_{Na} and P_K/P_{Na} were lower at pH 2.4 than at pH 7.4. We exploited this finding as a third source of variation in cation P's, by comparing P's at pH 7.4 and at low pH in frog and rabbit gallbladders. In the following paragraphs we characterize in detail the pH effect on conductance and p.d.'s. This characterization serves as background to describing on p. 293 the use of the pH effect as a source of variation in cation P's.

When serosal pH was lowered to 4.1, there was no change in dilution potentials or conductance of frog or rabbit gallbladders for up to 10 min. However, when mucosal pH was lowered to 4.1 (Fig. 4), conductance decreased to a new steady-state value with a half time of 30 ± 7 sec ($n = 6$) in rabbit and 22 ± 10 sec ($n = 6$) in frog. This half time is much longer than the value expected simply from diffusional delays for H^+ in the mucosal unstirred layer (~ 0.5 sec for an unstirred layer of 100 μ and a H^+ diffusion coefficient of 7.2×10^{-5} cm^2/sec). The lack of effect of serosal pH is probably

Table 1. Reversible effect of pH on permeability ratios

Time (min)	pH	P_{Na}/P_{Cl}	P_{Na}/P_K	P_{NH_4}/P_K
10	7.4	2.70		
13	7.4		0.70	
25	7.4			1.10
41	4.1	1.55		
46	4.1		0.82	
50	4.1			1.30
62	7.4	3.05		
68	7.4		0.71	
73	7.4			1.09

All measurements were made on a single frog gallbladder. The first column gives the elapsed time since mounting the preparation in the chambers; the second column, the bathing solution pH; the third column, P_{Na}/P_{Cl} calculated from measurement of a NaCl dilution potential; and the fourth and fifth columns, P_{Na}/P_K and P_{NH_4}/P_K calculated from measurement of a KCl:NaCl biionic potential and a NH_4Cl:NaCl biionic potential, respectively. Note that P_{Na}/P_{Cl} is lower, and P_{Na}/P_K and P_{NH_4}/P_K higher, at pH 4.1 than at pH 7.4; and that values at pH 7.4 are virtually the same before and after exposure to pH 4.1.

due to dissipation of the H^+ concentration gradient in the thicker serosal unstirred layer, and to the steepness of the pH-permeability relation in this pH range (Fig. 5).

To be certain that the effect of pH on permeability ratios is a reversible phenomenon rather than due to nonspecific damage, we measured conductance, biionic potentials, and dilution potentials at pH 7.4, repeated the measurements at after lowering both mucosal and serosal pH to some new value, repeated the measurements pH 7.4, and compared the values at low pH with the average of the two sets of values at pH 7.4. Provided that the exposure to low pH was sufficiently brief, the effect of pH on permeability ratios was completely reversible, as judged by comparison of dilution potentials or biionic potentials at pH 7.4 before and after exposure to low pH. For example, Table 1 presents the results of an experiment in bullfrog gallbladder, in which low pH reversibly decreased P_{Na}/P_{Cl} while increasing P_{Na}/P_K and P_{NH_4}/P_K.

Table 2 summarizes the effect of pH 4.1 solutions on total conductance and on partial ionic conductances. In both rabbit and frog, in either Cl^- or NO_3^- solutions, total conductance decreases on going from pH 7.4 to 4.1, by 36 to 47%. This decrease is due entirely to a decrease in G_{Na}, by 45 to 58% (59 to 70% decrease in $G_{Na}(m)$). There is no change in anion conductance (G_{Cl} or G_{NO_3}). Similar results were obtained in one experiment on a goldfish gallbladder. Fig. 4 illustrates the complete reversibility of these effects.

Table 2. Effect of low pH on gallbladder conductance

Species	Anion	pH	Total G	G_{Na} (shunt)	G_{Na} (membrane)	G_{Cl}	G_{NO_3}
Rabbit	Cl^-	7.4	39.9±2.7	3.8±1.0	30.4±3.7	5.7±1.6	–
		4.1	21.2±1.6	3.6±1.1	11.7±0.6	5.9±1.7	–
Rabbit	NO_3^-	7.4	38.1±2.9	5.8±1.3	24.0±2.0	–	8.3±1.8
		4.1	23.1±1.7	5.5±1.5	9.8±0.4	–	7.8±1.3
Frog	Cl^-	7.4	14.7±1.3	2.4±0.5	8.6±0.3	3.8±1.3	–
		4.1	9.0±0.8	2.3±0.6	2.9±0.2	3.8±1.0	–
Frog	NO_3^-	7.4	20.1±1.7	2.6±0.1	13.8±1.6	–	3.7±0.2
		4.1	10.7±0.4	2.8±0.1	4.0±0.5	–	3.9±0.2

Conductance units are mmho/cm^2. Each entry is an average value and standard error of the mean, based on three gallbladders. In each gallbladder, total conductance and dilution potentials were measured at pH 7.4, then at pH 4.1, and finally at pH 7.4 again, in NaCl or $NaNO_3$ Ringer's solution. As described on p. 282, the value of P_{Na}/P_{Cl} or P_{Na}/P_{NO_3} was used to resolve total G into the contributions of G_{Cl} or G_{NO_3}, G_{Na} in the shunt, and G_{Na} in native membrane. Since total G is assigned either to G_{Na} or to G_{anion}, the conductance associated with the small concentrations of K^+ ($G_K \sim 0.05\ G_{Na}$) is implicitly lumped with G_{Na}.

A more detailed picture of the pH effect emerges from use of a wide pH range to study the pH-dependence of the partial conductances G_{Na} and G_{Cl}, corrected for shunt conductance as discussed on pp. 281–282. (In the following paragraphs and Fig. 5 and Eqs. (8)–(12), we use for simplicity the symbols G_{Na} and G_{Cl} instead of our previous symbols $G_{Na}(m)$ and $G_{Cl}(m)$, to refer to these native membrane conductances corrected for shunt.) Fig. 5, above and below, displays the results for rabbit and frog gallbladders, respectively. It is immediately obvious that results for both species are very similar. G_{Na} remains constant from pH 9.5 down to about pH 6, then decreases sigmoidally with pH down to about pH 3 and levels off at a low value. In contrast, G_{Cl} remains negligible from high pH down at least to pH 3.8 but then *in*creases steeply down to at least pH 2.5.

The pH-dependence of G_{Na} is reminiscent of the titration curve of an acidic group. The experimental values were therefore fitted to an equation derived from the following two assumptions:

1. G_{Na} is assumed to be partly or totally controlled by a single, uniform population of membrane acidic groups, X, with a certain pK_a value. The relation between pH, the pK_a, and the concentrations of the charged form X^- and the neutral form XH is the usual equation

$$pH = pK_a + \log[(X^-)/(XH)]. \tag{8}$$

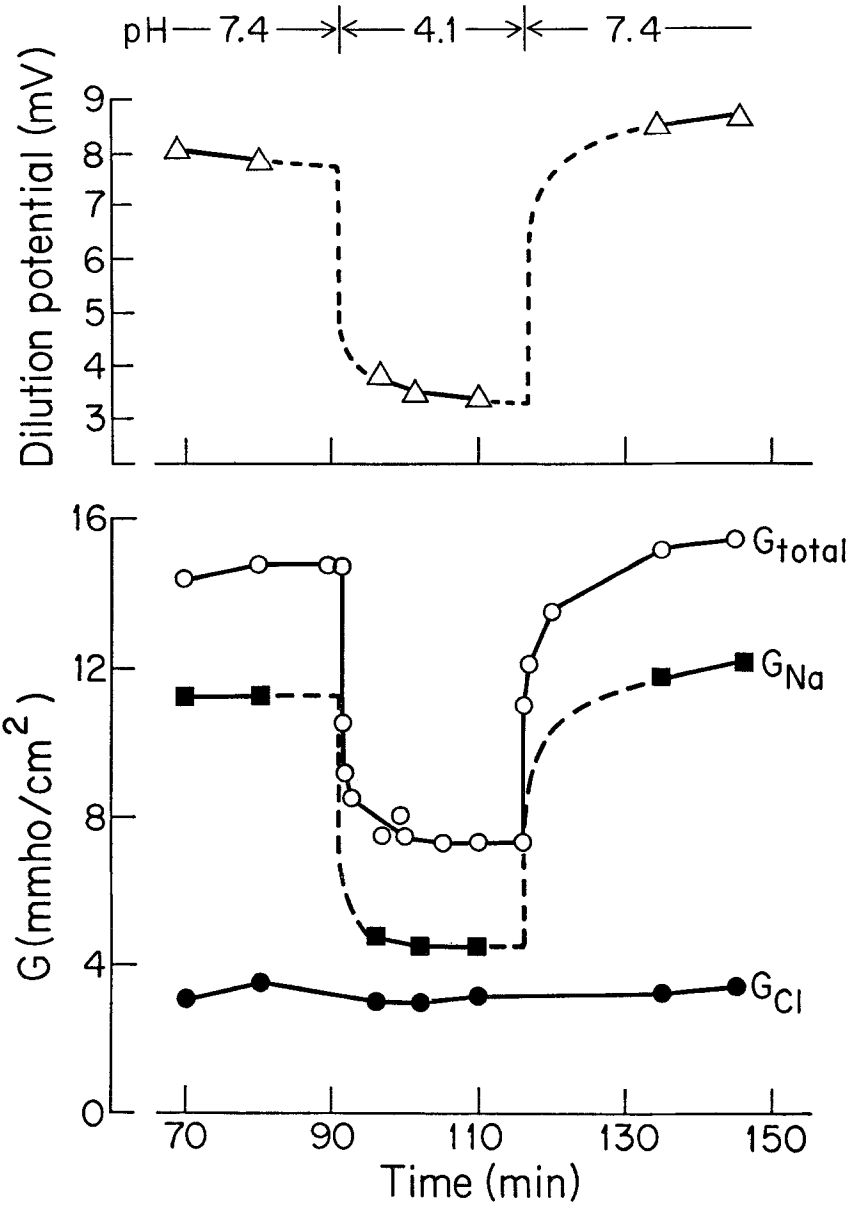

Fig. 4. Effect of low pH on 2:1 NaCl dilution potentials (△), total conductance (○), G_{Na} (□), and G_{Cl} (●) of a frog gallbladder. G_{Na} and G_{Cl} are not corrected for the shunt—i.e., they represent the sum of membrane conductance and shunt conductance. Between the arrows, mucosal and serosal pH was lowered to 4.1. Partial conductances were calculated from total G and from P_{Na}/P_{Cl} extracted from dilution potentials. The abscissa is the elapsed time from mounting the gallbladder between chambers. Note that the decrease in dilution potentials and the decrease in total G are due entirely to a decrease in G_{Na}

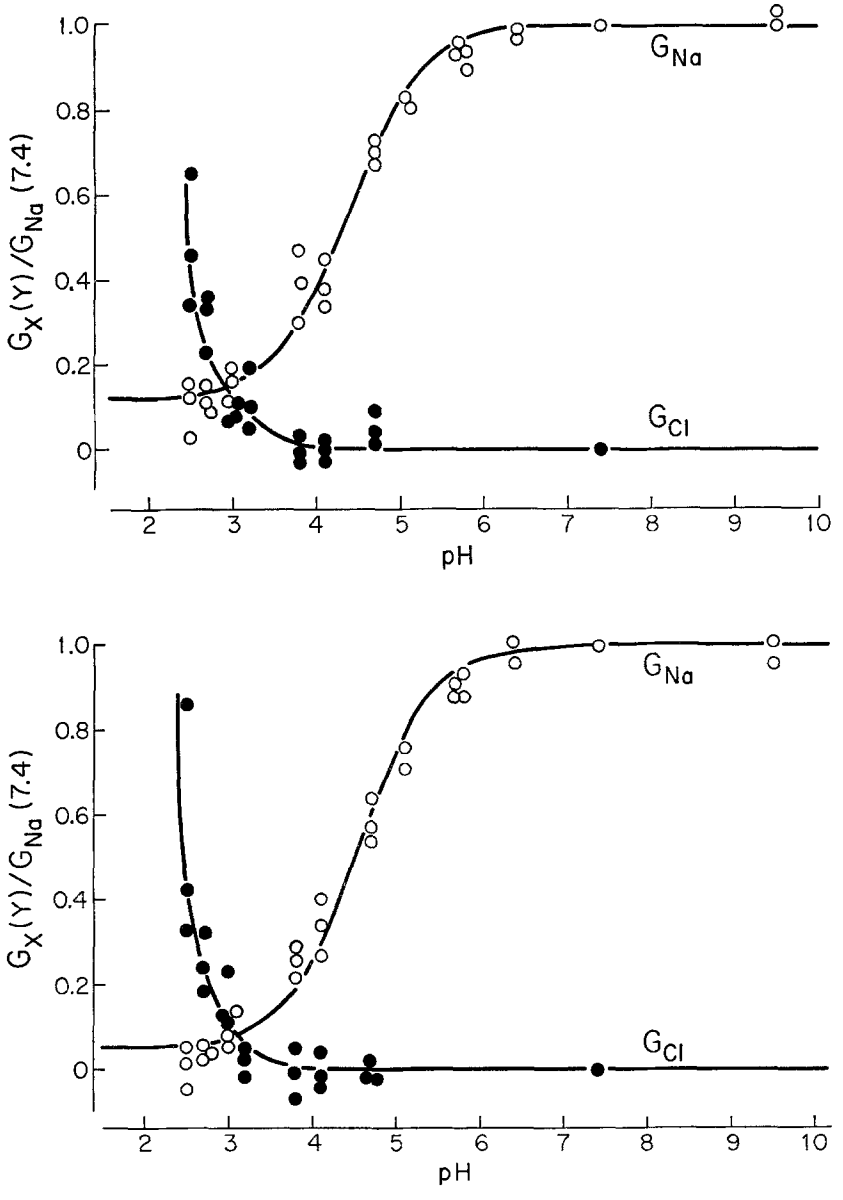

Fig. 5. Ordinate: conductance of Na^+ (○) or Cl^- (●) at the bathing solution pH given by the abscissa, divided by G_{Na} at pH 7.4. The experimental values refer to the conductance of native gallbladder (i.e., shunt conductance has been subtracted from the total measured conductance, both in the case of G_{Na} and G_{Cl}). The line through the G_{Na} values is the least-mean-squares fit to Eq. (12), while the line through the G_{Cl} values has been drawn by eye. The upper figure is for rabbit gallbladder, the lower for frog gallbladder. Note that G_{Na} values are well fitted by Eq. (12) with a pK_a near 4.6, implying that an acidic group controls cation permeation; that G_{Cl} is controlled by a group with a lower pK_a; and that rabbit and frog results are very similar

2. The Na^+ conductance controlled by these groups is assumed to be directly proportional to the number of groups in the charged form: i.e.,

$$G_{Na} = K(X^-) \tag{9}$$

for this component of G_{Na}, where K is a constant. If the pK_a lies sufficiently below 7.4 that virtually all the groups are in the charged form at pH 7.4 (i.e., $(XH)/(X^-) \sim 0$), as suggested by Fig. 5, then the equation

$$G_{Na}(y)/G_{Na}(7.4) = [1 + 10^{(pK_a - y)}]^{-1} \tag{10}$$

holds for this component of G_{Na}, where $G_{Na}(y)$ is the value of this component at a pH value of y.

In addition to this component of G_{Na} controlled by acidic sites, there might exist a pH-independent component of G_{Na}, termed G^0_{Na}. In this case the total Na^+ conductance would be given by

$$G_{Na} = G^0_{Na} + K(X^-). \tag{11}$$

The resulting equation is

$$\frac{G_{Na}(y)}{G_{Na}(7.4)} = \frac{G^0_{Na}}{G_{Na}(7.4)} + \left[\left(1 - \frac{G^0_{Na}}{G_{Na}(7.4)}\right)(1 + 10^{pK_a - y})^{-1}\right]. \tag{12}$$

Since G^0_{Na} could be zero, Eq. (12) includes Eq. (10) and is more general than it.

The curves drawn through the experimental G_{Na} values of Fig. 5 are based on a least-mean-squares fit of the experimental values to Eq. (12). The fitted parameters and their standard deviation are: $pK_a = 4.39 \pm 0.04$ for frog, 4.55 ± 0.04 for rabbit; $G^0_{Na}/G_{Na}(7.4) = 0.05 \pm 0.01$ for frog, 0.12 ± 0.01 for rabbit.

Thus, the observed pH-dependence of G_{Na}, and the good fit of the experimental values of Fig. 5 to Eq. (12), are consistent with the following interpretation:

Most or nearly all of G_{Na} could be controlled by a single population of acidic groups.

There is no obvious indication of cooperative interactions among these groups in their pK_a values, since this would distort the fit of Eq. (12) to the experimental values of Fig. 5.

This component of G_{Na} is directly proportional to the number of acidic groups in the charged form.

The small difference between apparent pK_a values for frog and rabbit is probably not significant.

G^0_{Na} is apparently not quite zero: i.e., there may still be a small Na^+ conductance left when all the acidic groups are protonated.

The sites responsible for increased G_{Cl} at low pH have a much lower apparent pK_a than the sites controlling G_{Na} with an apparent pK_a near 4.39 to 4.55. Since G_{Cl} is still increasing steeply with decreasing pH at pH 2.5 and shows no signs of approaching an asymptote, we cannot estimate how far below 3 is the pK_a of the Cl^--controlling sites.

The likely molecular interpretation of the acidic site is that it is either a carboxyl group ($-COO^- \overset{H^+}{\rightleftarrows} -COOH$) or phosphate

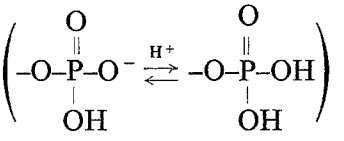

with a pK_a between 4 and 5, so that the negative charge disappears by protonation at lower pH values.

The increase in G_{Cl} at lower pH is presumably due to the protonation of an amine or some other nitrogen function ($—NH_2 \overset{H^+}{\rightleftarrows} —NH_3^+$). In agreement with this interpretation is the effect of 1,5-difluoro-2,4-dinitrobenzene (FFDNB), a reagent that removes positive charge by reacting with an ionizable hydrogen of an amino group and other groups (Berg, Diamond & Marfey, 1965: $R—NH_2 + F—C_6H_3(NO_2)_2 \rightarrow R—NH—C_6H_3(NO_2)_2 + HF$, where R is any radical). Reaction of rabbit gallbladder with FFDNB reduces the magnitude of the anion-selective KCl dilution potential at pH 2.4, as expected if the enhanced G_{Cl} at this pH arises from a protonated amino group (Wright & Diamond, 1968).

Thus, over a wide range of pH values there are well-defined and readily interpreted changes in cation and anion conductance. In further experiments we explored the effect of the pH range 3.2 to 7.4 on the cation-to-cation permeability ratio P_{Na}/P_K in frog and rabbit gallbladders. As illustrated in Fig. 6, the ratio increases with decreasing pH for both species, the effect being more marked in rabbit than in frog. P_{Na}/P_K is lower than the free-solution mobility ratio u_{Na}/u_K at pH 7.4 in rabbit but higher than u_{Na}/u_K at acidic pH's, while P_{Na}/P_K exceeds u_{Na}/u_K at all pH values in frog.

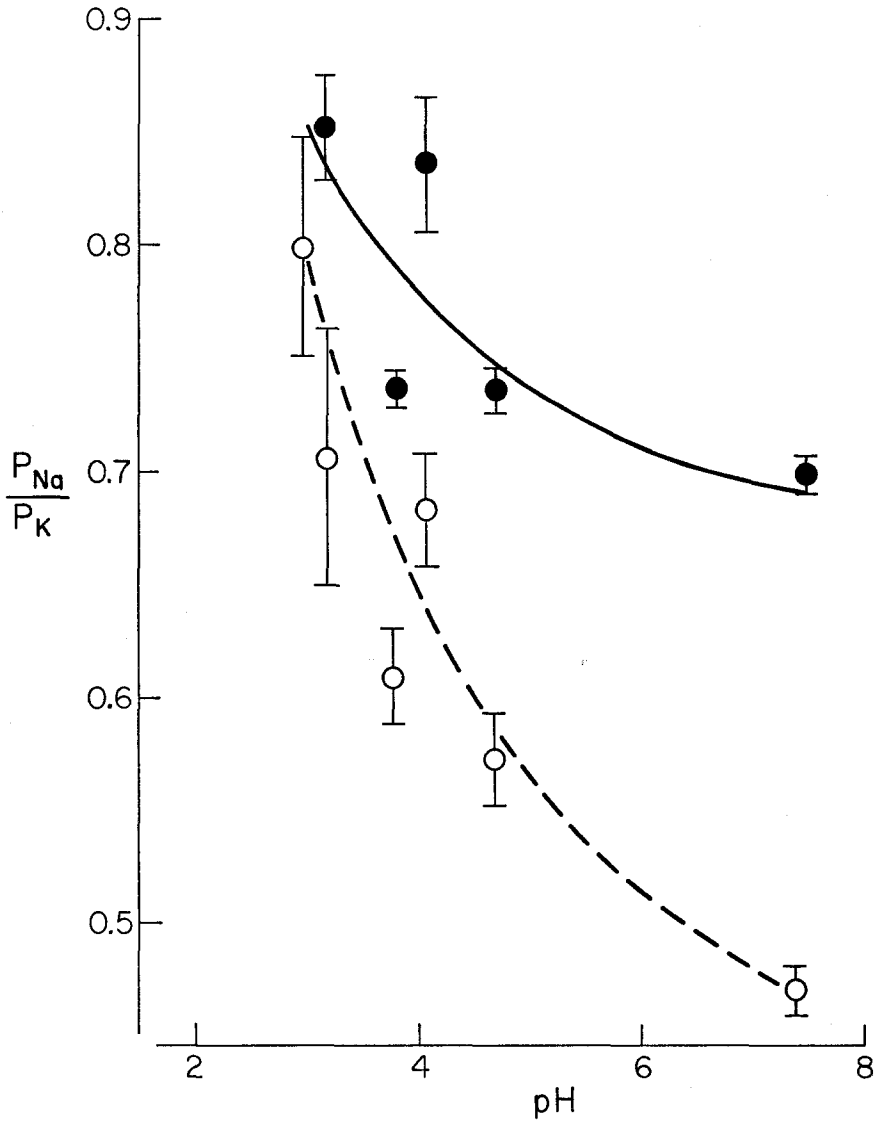

Fig. 6. P_{Na}/P_{Ka} as a function of bathing solution pH, in frog (•) and rabbit (○) gallbladder. Each point and the vertical bars give the average value and standard error of the mean for at least three different gallbladders. All P_{Na}/P_K values at a pH other than 7.4 have been normalized to the average value at pH 7.4, to minimize effects of variation between different gallbladders

In seven gallbladders tested (three from rabbit, three from frog, one from goldfish) P_{Na}/P_K was higher at pH 4.1 than at pH 7.4 in every case, and P_{NH_4}/P_K higher in six cases. These experimental results are given by the comparison of the closed and open symbols in Figs. 1, 2, 3 and 7.

Construction of Isotherms

In three frog gallbladders and three rabbit gallbladders we measured biionic potentials of all six test cations (Li^+, K^+, Rb^+, Cs^+, NH_4^+ and Tl^+) against Na^+, first at pH 7.4, then at 4.1, then at 7.4, and in some cases repeating both sets again. Fig. 7 gives isotherms for all cations in each species, constructed in the same manner as the NH_4^+ isotherms of Figs. 1–3. Table 3 summarizes average values of P for each cation in each species at each pH.

From Fig. 7 and Table 3, the following conclusions may be drawn:

A decrease in pH affects P of almost every cation. This can be seen most clearly in Fig. 7, by comparing P_X/P_K at pH 7.4 and 4.1 in the same animal. In some cases the quantitative changes in P_X/P_K at low pH are sufficient to produce inversions in the permeability sequence. At pH 7.4 the sequence in frog gallbladder is $Tl^+ > NH_4^+ > Rb^+$, $K^+ > Cs^+ > Na^+ > Li^+$. At pH 4.1 the positions of Cs^+ and Na^+ are reversed in all frogs. In rabbit gallbladder the sequence at pH 7.4 is $K^+ \geqq Tl^+ > Rb^+$, $NH_4^+ > Na^+ > Li^+ > Cs^+$. The positions of Tl^+ and K^+, NH_4^+ and Rb^+, and NH_4^+ and K^+ reverse at pH 4.1 in some rabbits. We did not observe a Cs^+/Na^+ inversion, as Wright and Diamond (1968) reported for rabbit gallbladder. This difference could be because they used a lower pH (2.4) or because they did not correct for the shunt.

In a given species at a given pH, there is individual variation in P of a given cation, and variations in different cations tend to be correlated. In most cases it is clear that P for a given ion at pH 4.1 deviates from P at

Table 3. Average values of relative permeability coefficients

Cation	Rabbit		Frog	
	pH 7.4	pH 4.1	pH 7.4	pH 4.1
Li^+	0.47±0.01	0.60±0.05	0.41±0.03	0.43±0.04
Na^+	0.52±0.02	0.75±0.04	0.70±0.04	0.83±0.01
K^+	1.0	1.0	1.0	1.0
Rb^+	0.76±0.02	0.87±0.03	1.03±0.02	1.03±0.01
Cs^+	0.30±0.01	0.43±0.01	0.78±0.04	0.80±0.01
NH_4^+	0.74±0.04	1.01±0.04	1.16±0.06	1.26±0.02
Tl^+	0.94±0.10	1.35±0.12	1.27±0.06	1.46±0.05

Each entry is an average value and standard error of the mean, based on three gallbladders, of the permeability coefficient relative to $P_K = 1$. The values were obtained by calculating P_X/P_{Na} (corrected by Eq. (7) for effects of the shunt) from the X:Na biionic potential, averaging the values for an individual animal at one pH, and dividing by the average value of P_K/P_{Na} for the same animal at the same pH.

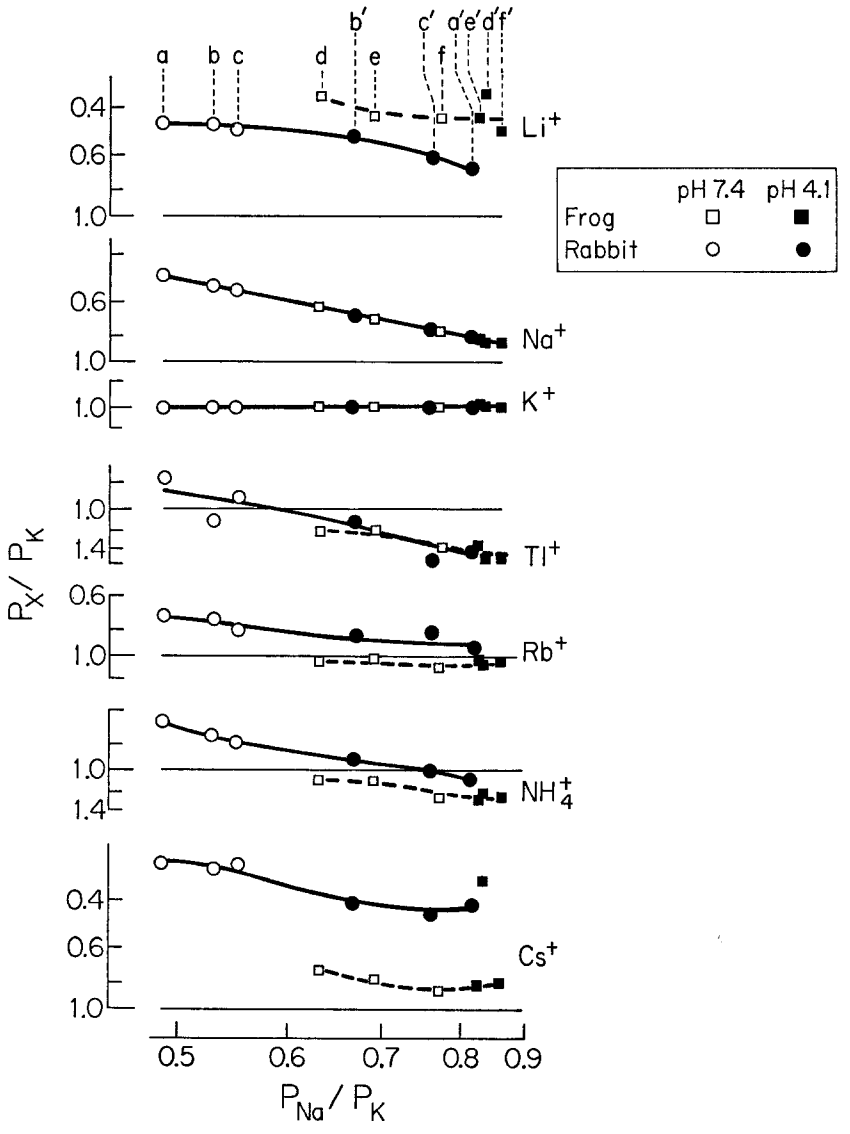

Fig. 7. Isotherms for seven monovalent cations in frog and rabbit gallbladders, constructed in the same manner as Fig. 1. The experimental points for each ion are plotted together with the second-order polynomial fitted through the points for each species by least-mean-squares (solid curve, rabbit; dashed curve, frog; frog curve identical to rabbit curve in the cases of K^+ and Na^+). Each ion was measured at pH 7.4 (○) and 4.1 (●) in each of three rabbits, identified by the letters *a*, *b* and *c*, and at pH 7.4 (□) and 4.1 (■) in each of three frogs, identified by the letters *d*, *e* and *f*. Thus, sets of seven points along the same imaginary vertical line were measured in the same animal at the same pH; and the two sets of points identified by the same letter were measured in the same animal at different pH's, the unprimed points (*a*, *b*, etc.) at pH 7.4, the primed points (*a′*, *b′*, etc.) at pH 4.1

pH 7.4 in the direction predicted by extrapolating the P_X/P_K isotherm, based on individual variation at pH 7.4, in the direction along the abscissa specified by the value of P_{Na}/P_K at pH 4.1. This is particularly obvious in the case of NH_4^+, the ion on which we made the most measurements (Figs. 1 and 2). In frog gallbladder, P_{NH_4}/P_K in frogs with the highest values at pH 7.4 actually overlaps the values in other frogs at pH 4.1 with the same value of P_{Na}/P_K (Fig. 1). Thus, variation due to pH is simply a quantitative extension of the effects manifested in individual variation at pH 7.4.

For each ion, measurements based on frogs and on rabbits define approximately but not exactly the same isotherms (Fig. 7). In general, permeability ratios in rabbits at pH 4.1 are similar to those in frogs at pH 7.4. The agreement between rabbit at pH 4.1 and goldfish at pH 7.4 may be even closer (Fig. 3).

Fig. 7 summarizes the *empirical* correlations between variation in P_X/P_K for one cation and variation in P_X/P_K for any other cation. These empirical correlations can be used as the basis for making predictions about permeability ratios in a new individual animal or at a new pH, once P_X/P_K has been measured for one cation in the new situation. For example, if P_{Tl}/P_K is measured in a certain rabbit at pH 6 and found to have the value of 1.10, then P_{Cs}/P_K is predicted to have a value of 0.52 in this particular rabbit at this particular pH. The prediction is made by locating $P_X/P_K = 1.10$ on the rabbit isotherm for Tl^+, drawing a vertical line through this point intersecting the Cs^+ isotherm, and reading off the value $P_X/P_K = 0.52$ from the ordinate.

Steric Restrictions on Permeating Cations

Close examination of Fig. 7 indicates a consistent trend in the differences between frog and rabbit. If one compares frog and rabbit values of P_X/P_K for a given ion at the same value of P_{Na}/P_K, the ion exhibiting the most marked difference between the two animal species is Cs^+: P_{Cs}/P_K values for rabbit are significantly lower than frog values (i.e., they lie above the frog values in Fig. 7). For NH_4^+ (*see also* Fig. 3) and Rb^+ there is a smaller discrepancy in the same direction; for Tl^+, almost no discrepancy. For K^+ and Na^+, the reference ions, there is by definition no discrepancy. For Li^+ the discrepancy is in the opposite direction (frog values lower than rabbit values). In order to depict these discrepancies quantitatively and graphically, we fitted second-order polynomials by least-mean-squares through the points for each ion in each species. Next, we read off from the ordinates the value of P_X/P_{Li} for each species at the value $P_{Na}/P_K = 0.75$ on the abscissa (half-way between the highest and lowest values of P_{Na}/P_K measured in the frog). Finally, from

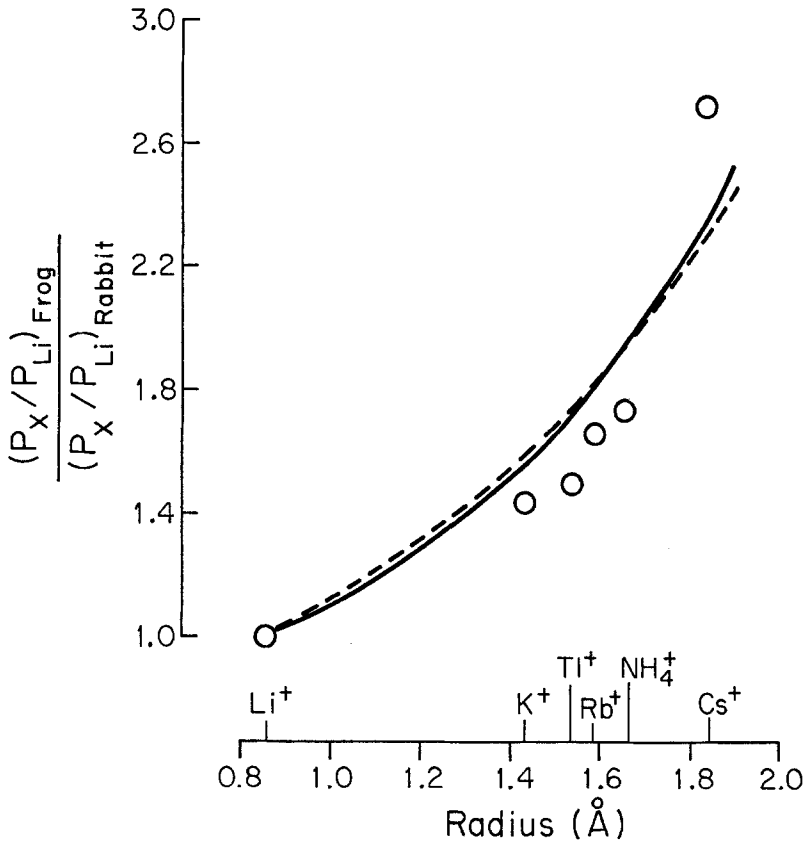

Fig. 8. Abscissa: Ladd ionic radius for each of six cations. Ordinate: the ratio $F_X \equiv (P_X/P_{Li})_{frog}/(P_X/P_{Li})_{rabbit}$ for the cation, based on P values read off the experimental isotherms (Fig. 7) at $P_{Na}/P_K = 0.75$. The dashed curve is the least-mean-squares fit of the Renkin formula [Eq. (13)] $(Y_{Li}/Y_X)_{rabbit}$, yielding $R_{rabbit} = 6.6$ Å. The solid curve is the least-mean-squares fit of the Renkin formula $(Y_X/Y_{Li})_{frog}/(Y_X/Y_{Li})_{rabbit}$, yielding $R_{rabbit} = 3.8$ Å, $R_{frog} = 5.9$ Å

these values of P_X/P_{Li} we calculated the ratio $F_X = (P_X/P_{Li})_{frog}/(P_X/P_{Li})_{rabbit}$ for each ion. Fig. 8 plots the values of F_X for each ion aganist the Ladd ionic radius (Ladd, 1968). It is obvious that F_X increases monotonically with ionic size, from 1.0 for the smallest cation, Li^+ (0.86 Å radius), to 2.74 for the largest ion, Cs^+ (1.84 Å radius). Qualitatively the same conclusion is reached if Pauling radii are substituted for Ladd radii, or if P_X/P_{Li} values are read off at the highest or lowest values of P_{Na}/P_K rather than at an intermediate value. The small discrepancies between the frog and rabbit isotherms of Fig. 7 may thus be expressed as follows: the larger the ion, the further its permeability in rabbit lags behind its permeability in frog.

This pattern suggests as an obvious interpretation that the patterns of cation selectivity in frog and rabbit gallbladders differ chiefly in that the pore in the tight junctions, through which ions must permeate (Barry *et al.*, 1971; Frömter, 1972; Frömter & Diamond, 1972), is narrower in rabbit than in frog. Independent evidence for a narrower pore in rabbit is provided by analysis of permeability to organic cations of different sizes (Moreno & Diamond, 1974*b*). To evaluate this interpretation, we applied the Renkin equation, which describes steric restriction to permeation in rigid, right-circular-cylindrical pores (Renkin, 1954):

$$Y_X \equiv (A_X/A) = [1-(r_X/R)]^2 [1-2.104(r_X/R)+2.09(r_X/R)^3-0.95(r_X/R)^5]; \quad (13)$$

where r_X is the radius of the permeating solute species X, R the radius of the pore, A the cross-sectional area of the pore ($=\pi R^2$), and A_X the effective area available for permeation of the solute. $Y_X=(A_X/A)$ is the factor by which the solute's permeability coefficient is reduced, compared to the value that would exist in the absence of any steric restriction and that would be determined solely by the physical variable underlying individual and pH variation (pp. 300–303). The hypothesis to be tested is that $(Y_X/Y_{Li})_{frog}/(Y_X/Y_{Li})_{rabbit}$ equals the factor F_X of Fig. 8. As the simplest model, we first assumed that steric restriction in the frog is negligible (i.e., $R_{frog}=\infty$, $Y_X(\text{frog})=1$ for all ions), and calculated by least-mean-squares the value of R_{rabbit} that gave the best fit of the Renkin factor $(Y_X/Y_{Li})_{frog}/(Y_X/Y_{Li})_{rabbit}=(Y_{Li}/Y_X)_{rabbit}$ to the F_X values of Fig. 8. The result (dashed curve, Fig. 8) was that R_{rabbit} equals 6.6 Å, with a standard deviation of 0.3 Å and mean-square error of 0.7 in F_X. As a slightly more complex model, we assumed that the pore radius in the frog is larger than in the rabbit but not infinite, and calculated by least-mean-squares the values of R_{frog} and R_{rabbit} that gave the best fit of $(Y_X/Y_{Li})_{frog}/(Y_X/Y_{Li})_{rabbit}$ to F_X. The result (solid curve, Fig. 8) was: $R_{rabbit}=3.8$ Å (SD 0.1 Å), $R_{frog}=5.9$ Å (SD 0.3 Å), mean-square error of 0.6 in F_X.

The actual numerical values obtained from these calculations of pore radii should not be stressed, because of uncertainties concerning the actual shape and rigidity of the channel, the relative importance of equilibrium and mobility factors in selectivity, the applicability of the Renkin equation to small charged molecules in narrow pores, etc. The point of the calculation is simply to confirm that the pattern of second-order differences between the frog and rabbit isotherms is approximately what one would expect if the permeation pathway in the rabbit offered greater steric restriction. At least the order of magnitude of the estimated radii is reasonable, for two reasons:

permeabilities measured for organic cations of different sizes yield similar estimates (Moreno & Diamond, 1974*b*); and the estimated radii are wide enough that ion interactions with channel ligands would be occurring in the presence of numerous water molecules, as also suggested by other features of the isotherms (*see* p. 308). It should be emphasized that this analysis of the second-order steric differences between frog and rabbit gallbladders is possible only because the much larger species differences due to differences in anionic field strength have already been taken into account, by interpolating frog and rabbit isotherms to the same value of P_{Na}/P_K and hence presumably of field strength.

Summary of Variation in Permeability Ratios

The permeability of each cation varies among individual animals, as a function of pH, and between species. The isotherms at low pH are simply an extension of the isotherms constructed from individual variation, and in some cases the permeabilities of one individual at one pH can be matched with those of another individual at another pH. The conclusion is that whatever factor varies between individuals to produce their differences in P's is also the factor that varies with pH to produce differences in P's. Furthermore, the approximate agreement between isotherms from different species means that permeability differences between species must arise to a large degree simply from average differences in this same factor. Individuals of one species can often be matched with individuals of another species, at the same pH or at a different pH, in their P's. Superimposed on this average species difference in the factor responsible for individual variation and pH-dependence are second-order effects, arising from greater steric restriction in rabbit than in frog to larger ions. Finally, the variations in different ions are correlated, such that the selectivity isotherms can be used to predict empirically the permeability coefficient for any ion in a given individual at a given pH, once the permeability coefficient of any other ion under the same conditions has been measured. The conclusion is that variation in the same factor is responsible for variation in permeabilities of all the cations studied in the gallbladder. The identity of this factor is considered in the Discussion.

Discussion

We consider four problems of interpretation raised by these results: the origin of alkali cation selectivity; the mechanism of the pH effect on con-

ductance and selectivity; the origin of Tl^+ and NH_4^+ selectivity; and differences between gallbladder isotherms and those for other ion-selective systems.

Origin of Equilibrium Selectivity for Alkali Cations[2]

Marked differences among the alkali cations in permeability are observed not only in gallbladder but also in most other biological membranes and in artificial membranes, such as glass electrodes, collodion membranes, and carrier-doped thin lipid membranes. Specific effects of alkali cations are also noted in studies of enzyme activation, binding to colloids, binding to ion-exchange resins, and numerous other natural processes. Although the five alkali cations can be permuted in $5!=120$ different sequences, Eisenman (1961, 1962, 1965*a*) noted that only certain of these sequences recurred in nature as selectivity sequences, suggesting a common origin of selectivity in most systems. The permeability sequence in rabbit gallbladder, $K^+ > Rb^+ > Na^+ > Li^+ > Cs^+$, also characterizes the glass electrode NAS 28.3–9.7 (Eisenman, 1962). The permeability sequence at pH 7.4 in frog gallbladder, $Rb^+ \sim K^+ > Cs^+ > Na^+ > Li^+$, also characterizes the glass electrode NAS 27.2–7.8 (Eisenman, 1962), valinomycin-doped bilayers, monactin-doped bilayers, stimulation of the phosphatase from gastric mucosal microsomes, transport affinities in yeast, and stimulation of urine flow in *Calliphora* malpighian tubules (data summary by Diamond & Wright, 1969).

Eisenman reasoned that selectivity sequences could be related to differences among cations in values of $\Delta F_{\text{transfer}}$, the free-energy change in transferring the cation from water to the membrane sites that control permeation. For each cation one can write

$$\Delta F_{\text{transfer}} = \Delta F_{\text{ion/site}} - \Delta F_{\text{hydration}}, \tag{14}$$

where $\Delta F_{\text{hydration}}$ is the ion's hydration energy and $\Delta F_{\text{ion/site}}$ is the interaction energy between the ion and the membrane sites. For relatively nondeformable, nonpolarizable ions (like the alkali cations) and sites, $\Delta F_{\text{ion/site}}$ is likely to be dominated simply by the electrostatic attractive forces implicit

2 For discussion of evidence indicating that equilibrium selectivity generally makes a larger contribution than nonequilibrium selectivity (e.g., mobility differences) to permeability differences among alkali cations in biological membranes, *see* Diamond & Wright, 1969, pp. 609–612, and Moreno & Diamond, 1974*b*.

in Coulomb's law.[3] The sites in biological systems are almost certain to be oxygen ligands with a partial or full negative charge. For a given ion of given radius and charge, $\Delta F_{\text{ion/site}}$ thus depends on the effective site charge, site radius, and coordination number (i.e., number of oxygen atoms surrounding each cation). By varying site field strength through variation in either charge, radius, or coordination number, calculating $\Delta F_{\text{ion/site}}$ from Coulomb's law, and using experimental values of $\Delta F_{\text{hydration}}$, Eisenman obtained 11 sequences of $\Delta F_{\text{transfer}}$, which proved to be the selectivity sequences actually observed in most biological and nonliving systems. Sequence XI ($Li^+ > Na^+ > K^+ > Rb^+ > Cs^+$) arises from the strongest sites, sequence I ($Cs^+ > Rb^+ > K^+ > Na^+ > Li^+$) from the weakest sites. The permeability sequence of frog gallbladder, $Rb^+ \sim K^+ > Cs^+ > Na^+ > Li^+$, represents either Eisenman's sequence III ($Rb^+ > K^+ > Cs^+ > Na^+ > Li^+$) or IV ($K^+ > Rb^+ > Cs^+ > Na^+ > Li^+$), depending upon the relative positions of Rb^+ and K^+ in the particular frog studied. The sequence of rabbit gallbladder, $K^+ > Rb^+ > Na^+ > Li^+ > Cs^+$, differs from Eisenman's sequence V only in the reversed positions of Cs^+ and Li^+, due presumably to steric restrictions to Cs^+ permeation in the tight junctions of rabbit gallbladder.

This analysis implies that differences among gallbladders in their permeability ratios and sequences arise from differences in the effective electrostatic field strengths of the membrane oxygen ligands that are the nearest neighbors to permeating cations. These field strength differences probably reflect either small differences in coordination, or else differences in the partial negative charges on the oxygen ligands as a result of inductive effects of adjacent electron-withdrawing or electron-releasing groups. For instance, the quantitative differences among the carriers nonactin, monactin, dinactin, and trinactin in their permeability or binding ratios are in the direction expected from the electron-releasing effects of the added methyl groups by which the latter three carriers differ from nonactin (Szabo, Eisenman & Ciani, 1969). Similarly, progressive methylation of substituted formamide derivatives shifts their cation selectivity pattern in the direction from sequence I towards sequence XI, as expected for an increase in field strength from the inductive effect of the methyl groups (Krasne & Eisenman,

3 While Coulomb forces will always be important for alkali cations, and theoretical calculations of selectivity based on Coulomb forces alone are remarkably successful for most systems, other forces may require consideration in very tight systems. For example, with some macrocyclic carriers the differences in deformation energy for forming complexes with different ions may be important. Steric considerations in a tight cavity such as that of valinomycin may dictate whether or not a water molecule is included in the cavity along with a small ion, thereby greatly altering the equilibrium constant. *See* Grell, Funck and Eggers (1971) for further discussion.

1973, Fig. 46). The shift from sequence III to sequence V, i.e. from right to left along the gallbladder isotherms of Figs. 3 and 7, would correspond to an increase in effective field strength of the sites. Thus, we assume that individual frogs and rabbits with *higher*-than-average values of P_{Na}/P_K have sites with *lower*-than-average (sic) field strengths; and that rabbits, on the average, have stronger sites than frogs.[4] If these species differences in effective field strength were due to differences in partial negative charge on each oxygen ligand, a species difference in site pK_a would be expected (*cf.* Eisenman, 1962, Fig. 15). Our measurements (Fig. 5) do not detect a pK_a difference between frog and rabbit. This could be either because our estimate of pK_a is insufficiently accurate, or because the species differences in field strength are due to differences in coordination number.

Effect of pH

In every individual animal studied, the shifts in gallbladder permeability ratios with decreasing pH are in the direction from left to right along the isotherms of Fig. 7; i.e., from high-field-strength sequences towards low-field-strength sequences. Thus, rabbit gallbladder values, which are near sequence V at pH 7.4, shift at pH 4.1 towards the values observed in frog gallbladder at pH 7.4, which define sequence II or IV. Similarly, the selectivity sequences of glass electrodes (Eisenman, 1962, Fig. 3), of colloidal stearate derivatives (Teunissen, Rosenthal & Zaaijer, 1938: *see* Diamond & Wright, 1969, p. 592), and of frog skin (Pesente, 1969, Tables 1 and 2) shift in the direction from sequence XI towards I with decreasing pH.

The proton's positive charge will reduce the effective charge and hence the field strength of negatively charged sites. As discussed in the preceding section, equilibrium selectivity considerations predict a shift from sequence XI towards I with decreasing site field strength. Thus, the observed effects of pH on selectivity of gallbladders and other systems are in striking agreement with the postulated role of site field strength in controlling selectivity. Effects of pH on selectivity are expected no matter where the negative charges associated with the rate-limiting step for permeation are located, even if they are surface charges.

A problem remains in picturing exactly how protons reduce the effective charge of a site without altogether neutralizing it and eliminating it as

4 This assumption follows from the fact the P_{Na}/P_K decreases as one proceeds from sequence III to sequence V (right to left) along the gallbladder isotherms. In sets of isotherms that extend beyond sequence V, based on other epithelia (Barry *et al.*, 1971, Fig. 7), glass electrodes (Eisenman, 1965*a*, Fig. 7), or cell membranes and enzymes (Eisenman, 1965*a*, Fig. 8), the slope of the Na^+ isotherm changes sign beyond sequence V, so that an increase in P_{Na}/P_K corresponds to an increase in field strength.

a source of cation selectivity (e.g., because of protonating a $-COO^-$ group). If one imagined a site as capable of existing in only two possible forms, protonated or not protonated (e.g., $-COO^-$ or $-COOH$), then only two values of field strength and two selectivity sequences would be expected. Some suggested interpretations are as follows. (a) A proton comes on and off a site many times while an alkali cation is in the vicinity, so that the cation sees a time-averaged site of lower strength. (b) A site consists of several adjacent oxygen ligands contributing a total of more than one electron charge, so that a proton reduces but does not eliminate the net negative charge. A closely related alternative hypothesis is that the fields of adjacent sites overlap. (c) Sites with different pK_a values coexist within the channel. As pH is reduced, sites with the highest pK_a values (and highest field strengths) are protonated first, leaving sites with lower pK_a values and lower field strengths controlling selectivity. (d) The properties of a site depend on the state of its neighbors. For example, protonation of one site could alter the pK_a of adjacent sites by an inductive effect. The fit of the experimental points of Fig. 5 to Eq. (12) fails to provide obvious support for interpretations (c) or (d).

Origin of Tl^+ *and* NH_4^+ *Selectivity*

Tl^+ and NH_4^+ differ from the alkali cations in that an ionic model based on a nonpolarizable, nondeformable sphere with a point charge at the center is likely to provide a poor basis for predicting how these ions interact with ligands.

In the case of Tl^+, the ionic polarizability – i.e., the degree to which the ion's electron distribution is distorted by an applied electric field – is greater than that of any of the alkali cations (Pauling, 1927). Interactions of Tl^+ with ligands may also be stabilized by partial electron transfer and by promotion of electrons to higher energy orbitals (Cotton & Wilkinson, 1972). Because of these additional energy terms, interaction energies involving Tl^+ generally exceed those predicted from its crystallographic radius and Coulomb's law. For example, its energies of solvation by water, propylene carbonate (Salomon, 1970), nonactin, and valinomycin (Krasne & Eisenman, 1973) all exceed the interpolated values for an alkali cation of comparable size.

In the case of NH_4^+, the positive charge is not concentrated on the central nitrogen but is distributed over all five atoms (Pauling, 1960). Furthermore, the hydrogens of NH_4^+ can "form hydrogen bonds" with suitably placed oxygen ligands – i.e., resonance forces and van der Waals forces contribute significantly to the energy of oxygen/hydrogen interaction, in addition to

the monopolar interactions calculated from the electrostatics of point charges. Since the four hydrogens of NH_4^+ are arranged tetrahedrally, a site with a corresponding tetrahedral array of four oxygen atoms would solvate NH_4^+ more strongly than would a differently arranged site that yielded the same solvation energy as the tetrahedral site for alkali cations. This sensitivity of NH_4^+ to spatial details of the site has been invoked to explain why the macrotetralide actins, with four tetrahedrally arranged oxygens, have a relatively stronger affinity for NH_4^+ than does valinomycin, with six octahedrally arranged oxygens (Eisenman *et al.*, 1973; Krasne & Eisenman, 1973).

Thus, whereas monopolar forces alone are likely to dominate alkali cation selectivity, nonmonopolar forces in addition could be significant for Tl^+ selectivity, and the site's spatial configuration in addition could be significant for NH_4^+ selectivity. *A priori*, variation in these special factors might have been more important than variation in monopolar interactions as the source of biological variation in Tl^+ and NH_4^+ selectivity. Had this been the case, experimental values for P_{Tl}/P_K or P_{NH_4}/P_K would have scattered at random when plotted as a function of P_{Na}/P_K. In fact, Tl^+ and NH_4^+ experimental values in rabbit and frog gallbladders define as neat isotherms as do the points for Li^+, Rb^+ and Cs^+ (Figs. 3 and 7). This is especially clear for NH_4^+, the ion for which we obtained the largest number of experimental measurements (Fig. 3). Therefore, the same variations in field strength which account for most of the individual and pH-dependent variation in alkali cation selectivity probably also account for most of the variation in Tl^+ and NH_4^+ selectivity.[5] Furthermore, Fig. 8 shows that the values of $F_X = (P_X/P_{Li})_{frog}/(P_X/P_{Li})_{rabbit}$ for $X = Tl^+$ or NH_4^+ fall on the same curve as that defined by the alkali cations, interpolated at the radii of Tl^+ of NH_4^+. Therefore, the differences between frog and rabbit in Tl^+ or NH_4^+ permeability are probably due to the same factors as those responsible for species differences in alkali cation permeability: viz., primarily, a species difference in site field strength, and secondarily, greater steric hindrance in the rabbit.

However, one could not conclude from this reasoning that field-strength considerations account for the *actual values* of P_{Tl}/P_K and P_{NH_4}/P_K; field strength simply accounts for the *variation* in P_{Tl}/P_K and P_{NH_4}/P_K. Fig. 9 plots $\Delta F_{hydration}$, $\Delta F_{transfer}$, and $\Delta F_{ion/site}$ for each cation, as a function of its ionic radius. It is clear that not only $\Delta F_{hydration}$ but also $\Delta F_{ion/site}$ for Tl^+ is greater than expected from its radius, in comparison to the alkali cations. Therefore,

5 There is no evidence to rule out the possibility that variation in non-monopolar forces or site geometry is coincidentally closely correlated with variation in field strength, but there is also no evidence to support this less likely and more complicated interpretation.

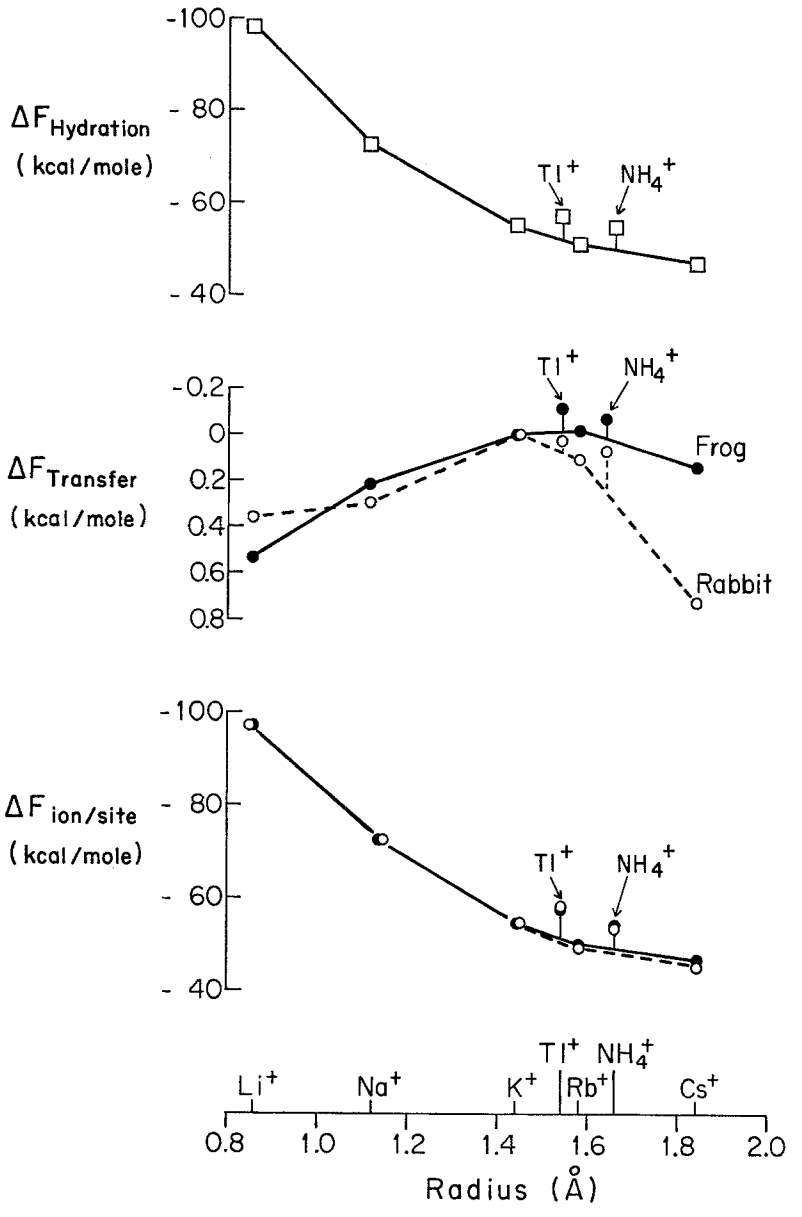

Fig. 9. Free energy of hydration (Salomon, 1970 for the alkali cations and Tl^+; estimated from $\Delta H_{hydration}$ and an assumed value of $\Delta S_{hydration}$ (intermediate between $\Delta S_{hydration}$ of Rb^+ and Cs^+) for NH_4^+), of transfer from water to gallbladder membrane sites, and of solvation by gallbladder membrane sites, as a function of ionic radius (Ladd, 1968), for monovalent cations. In each case the quantity plotted is ΔF for a given ion, minus the corresponding ΔF for Cs^+. $\Delta F_{transfer}$ was calculated as $-RT\ln(P_X/P_K)$, using the permeability ratios of Table 3. $\Delta F_{ion/site}$ was calculated as $\Delta F_{transfer}+\Delta F_{hydration}$. Note that, for both Tl^+ and NH_4^+, all three ΔF's are more negative than expected for an alkali cation of the same size

non-monopolar forces must be significant for Tl^+'s interactions not only with water but also with gallbladder membrane sites. Fig. 9 also suggests that this conclusion applies to NH_4^+. However, these non-monopolar forces apparently vary less among membranes from different individuals, among species, or with pH than do monopolar forces, since P_{Tl}/P_K and P_{NH_4}/P_K still correlate closely with P_{Na}/P_K.

Site Fingerprints

While alkali cation permeability sequences of most biological and artificial membranes are close to the set of 11 sequences predicted from Coulomb's law, there are quantitative differences among different groups of systems, such as glass electrodes compared to macrotetralide actin carriers (Eisenman *et al.*, 1973, Figs. 34–37). These differences are more marked for Tl^+ and NH_4^+, the ions for which nonmonopolar forces or the spatial array of ligands are most important. As pointed out by Eisenman *et al.* (1973), these differences probably reflect differences in site structure – i.e., whether the oxygens with which cations interact are in tetrahedral coordination (as in the actin carriers) or in sixfold coordination (as in the valinomycin carrier), or whether the oxygens are part of an ether linkage (as in polyether carriers), a carboxyl group (as in collodion), or an ester carbonyl group (as in valinomycin). Thus, these details of selectivity provide for the biological sites a "fingerprint" that can be compared to fingerprints for model systems of known structure, in order to estimate the molecular structure and configuration of the biological sites.

Fig. 10 gives the selectivity isotherms for glass electrodes in the region of sequences III through V, for comparison with the frog and rabbit gallbladder isotherms of Figs. 11 and 12. Fig. 13 gives P_X/P_K values for seven other "leaky" epithelia superimposed on the isotherms for frog and rabbit gallbladders. Selectivity data for various types of carriers are presented in Fig. 14 as graphs of log (P_X/P_K) against r_X (the ionic radius in Å), since not enough carriers of each type have been studied to construct isotherms.

Comparison of Fig. 10 with Figs. 11 and 12 shows that the glass isotherms and gallbladder isotherms agree well in shape and in relative positions of individual isotherms, even for Tl^+ and NH_4^+. The differences in position of the isotherm for Cs^+, the largest ion, are presumed due to differences in steric restriction, as suggested by Fig. 8. The most marked difference is that the magnitude of selectivity is much greater in glass than in gallbladder (note difference in ordinate scale of Fig. 10 compared to Figs. 11 and 12). For example, the permeability sequence is $K^+ > Rb^+ > Na^+ > Li^+ > Cs^+$ both in rabbit gallbladder and in the glass electrode NAS 28.3–9.7,

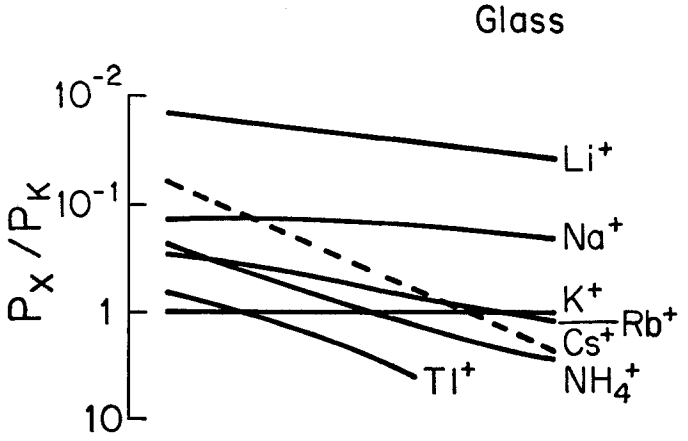

Fig. 10. Selectivity isotherms for glass electrodes in the region between sequences III and V (alkali cation isotherms after Eisenman, 1962, Fig. 8*a*; NH_4^+ and Tl^+ isotherms after Eisenman, 1965*b*, Fig. 35). The ordinate is P_X/P_K, the abscissa is P_{Na}/P_K, and the isotherms were constructed in the same manner as Figs 1, 2, 3 and 7

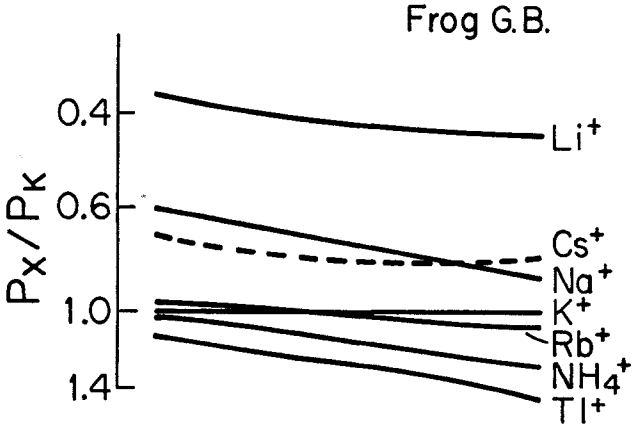

Fig. 11. Selectivity isotherms for frog gallbladder. The isotherms for each ion (*see* Fig. 7) have been redrawn together without the experimental points

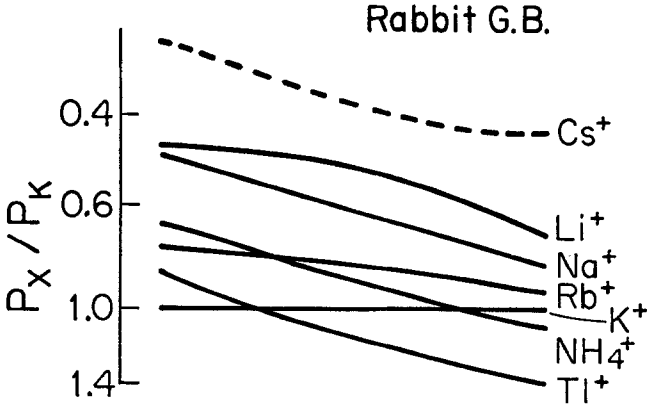

Fig. 12. Selectivity isotherms for rabbit gallbladder. The isotherms for each ion (*see* Fig. 7) have been redrawn together without the experimental points

but the relative permeabilities are 1.00:0.76:0.52:0.47:0.30 in the former; 1.00:0.55:0.37:0.03:0.02 in the latter. Gallbladder is also much less selective than model carriers of the K^+ channel of nerve (compare ordinates of Fig. 14). Analogous quantitative differences in model systems (Eisenman, 1962, Fig. 18) suggest as an interpretation that the permeation channel through gallbladder tight junction is more hydrated than in glass. This conclusion is in accord with other knowledge about tight junctions. The low selectivity and high hydration of gallbladder tight junction may be due to its relatively wide pore (estimated from the analysis of steric restriction), as compared to the narrower values of pore radius estimated for K^+ channel and Na^+ channel of nerve (Hille, 1971, 1973; Benzanilla & Armstrong, 1972). While the estimate of gallbladder pore radius is insufficiently accurate to merit stress, it is still interesting to note that a cross-section of the estimated pore would admit at least three water molecules in rabbit (more than three in bullfrog) in addition to the ion. In contrast, the K^+ and Na^+ channels of nerve have been estimated to admit not more than one water molecule in addition to the ion (Hille, 1971, 1973).

The seven epithelia whose P_X/P_K values are depicted in Fig. 13 include goldfish gallbladder, frog choroid plexus, rat proximal tubule, jejunum and ileum of rabbit, and intestine of goldfish and frog. In all these epithelia the high-conductance pathway is thought to be via junctions, as in rabbit and frog gallbladders; i.e., these tissues all exemplify "leaky" epithelia. The most striking feature of Fig. 13 is that all these epithelia have low permeability ratios, like rabbit and frog gallbladders but unlike nerve, glass or macrocyclic carriers. Thus, the junctions of all leaky epithelia may provide a hydrated permeation pathway. Among the epithelia, the points for goldfish gallbladder and frog and rabbit intestines lie closer to the frog gallbladder isotherms than to the rabbit isotherms. Guinea-pig gallbladder (illustrated in Fig. 3 but not in Fig. 13) has an especially low P_{Na}/P_K value, while rabbit ileum and goldfish gallbladder have especially high P_{Na}/P_K values. These findings suggest small differences among these tissues in steric restrictions and average value of field strength, superimposed on a general similarity in hydration.

Fig. 14 compares $\log(P_X/P_K)$ values for eight individual membranes, whereas Figs. 10–12 compared sets of isotherms, each set constructed from measurements on many related membranes. Fig. 14 suggests that, depending upon the chemical nature and spatial orientation of the ligands, the values of $\Delta F_{transfer}$ (*see* Eq. (14), p. 300) or of $\log(P_X/P_K)$ for Tl^+ or NH_4^+ may be either greater or less than ("supra-Ia" or "sub-Ia", in the terminology of Eisenman *et al.*, 1973) the value for an alkali cation (group Ia of the periodic table)

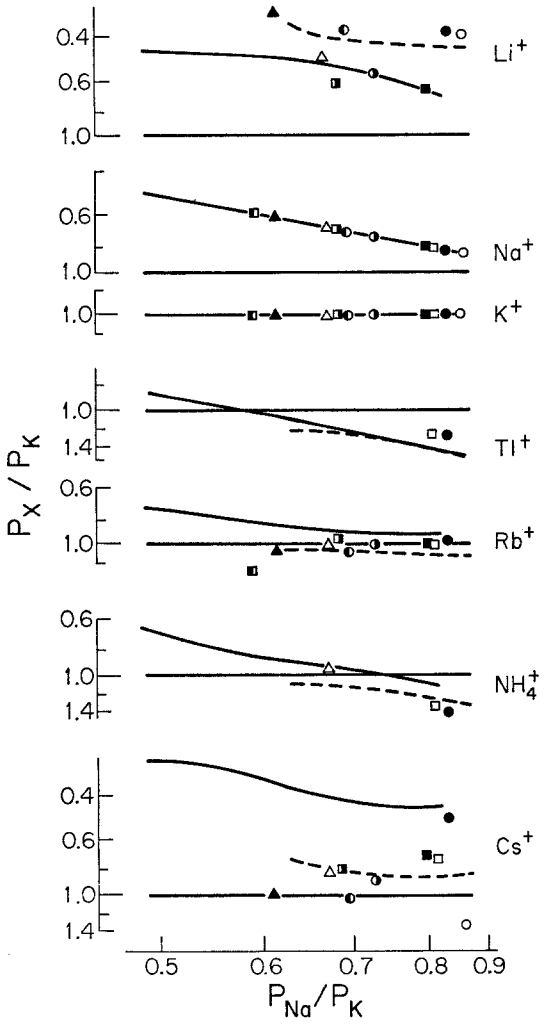

Fig. 13. Selectivity isotherms for monovalent cation permeation in "leaky" epithelia. The figure has been constructed in the same manner as Figs. 1–3 and 7, by plotting P_X/P_K for the given cation against P_{Na}/P_K measured in the same preparation under the same conditions. Thus, points located vertically above each other refer to different ions in the same preparation. The horizontal lines are the K^+ isotherm (P_X/P_K automatically equals 1.0), while the solid and dashed curves are the isotherms in rabbit and frog gallbladders, respectively, for the given ion, copied from Fig. 7. Experimental points are based on rabbit ileum (○; Frizzell & Schultz, 1972); rat jejunum (◧; B. D. Munck & S. G. Schultz, *personal communication*); choroid plexuses (■ & ◑) and intestines (▲ & ◐) from two individual frogs (Wright, 1972); rat proximal tubule (◨; E. Frömter, *personal communication*); goldfish gallbladder at pH 4.1 (●) and 7.4 (□), and goldfish intestine at pH 7.4 (△) (our measurements). The fact that values for the 10 other epithelia fall close to the isotherms for frog and rabbit gallbladders implies that the "tight" junctions of all these epithelia share similar selectivities and a similar degree of hydration

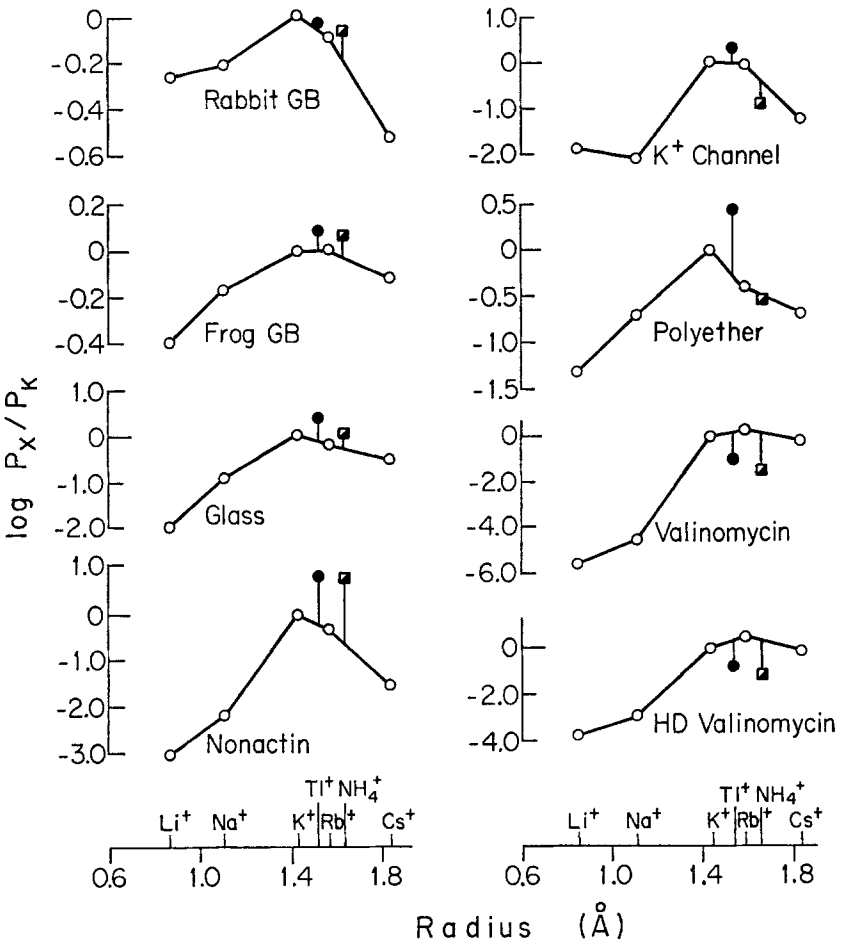

Fig. 14. Logarithms of cation permeability ratios P_X/P_K in various systems, plotted against Ladd ionic radius (Ladd, 1968). Note that permeabilities of alkali cations (○) are maximal at an intermediate ionic size; that NH_4^+ (◪) and Tl^+ (●) may deviate from the pattern defined by alkali cations in each system; and that the ordinates differ for different systems. Data sources: frog and rabbit gallbladders, Table 3 of this paper; glass electrode, Eisenman, 1962 and 1965*b*; hexadecavelinomycin (abbreviated HDvalinomycin), Eisenman and Krasne, 1973, Fig. 8; remaining systems, Krasne and Eisenman, 1973, Figs. 52 and 53

of comparable size. However, it is more difficult to draw reliable conclusions from the comparisons of Fig. 14 than from those of Figs. 10–12. The eight membranes of Fig. 14 differ in their alkali cation selectivity sequences (Eisenman sequences III, IV or V). The isotherms of Figs. 10–12 suggest that, within a group of related membranes with the same ligand species but

different field strengths, Tl^+ and NH_4^+ may each behave either as supra-Ia or sub-Ia, depending upon the alkali cation sequence exhibited and the value of P_{Na}/P_K (and presumably of field strength). Furthermore, comparable values of P_{Na}/P_K do not guarantee comparable values of field strength, because P_{Na}/P_K varies with degree of hydration among systems of similar field strength (Eisenman, 1962, Fig. 18). With these reservations, Fig. 14 shows (as discussed by Eisenman *et al.*, 1973, and by Krasne & Eisenman, 1973) that P_{NH_4} is considerably greater than expected for an alkali cation of comparable size ("supra-Ia") in nonactin, slightly greater in glass and gallbladder, somewhat less in a polyether, and considerably less in valinomycin, hexadecavalinomycin, and the K^+ channel of nerve. The strongly supra-Ia position of NH_4^+ with nonactin has been attributed to the interaction between the tetrahedrally arranged carbonyl ligands of nonactin and the tetrahedrally arranged protons of NH_4^+ (Eisenman *et al.*, 1973). P_{Tl} is greater than expected for an alkali cation of comparable size in all systems except valinomycin and hexadecavalinomycin, where it is considerably less.

The "fingerprint" of gallbladder in Fig. 14 is more similar to glass (and to collodion, which resembles glass: Eisenman, 1962, Fig. 8*a*), than to that of other systems. The macrocyclic carriers each consist of a single molecular species with a small number (4 to 8) of oxygen atoms arranged in a regular spatial array. Glass and collodion, however, are polymeric networks in which there is less regular spatial organization. The similarity of gallbladder to glass and collodion may therefore mean that there is also not a precisely repeating pattern to the arrangement of oxygen ligands in gallbladder tight junctions, and that gallbladder sites bear net charge.

It is a pleasure to acknowledge our debt to Drs. G. Eisenman, S. Krasne, and G. Szabo for suggestions and for criticism of the manuscript; and to Drs. N. Bindslev, E. Frömter, S. G. Schultz, G. Wiedner and E. M. Wright for permission to cite unpublished results. This work was supported by grant GM 14772 from the National Institutes of Health, and by a N.I.H. International Fellowship awarded to J.H.M.

Appendix

Potential Difference Transients

When nonelectrolyte is added to or removed from the solution on one side of the gallbladder, a p.d. ("streaming potential") builds up or decays with a half time proportional to the solute's diffusion coefficient in the unstirred layer adjacent to the gallbladder (Diamond, 1966, Fig. 3; Wright & Diamond, 1969, Fig. 1). P.d. transients resulting from changes in ion

concentrations are generally similar (*see* Diamond, 1962 and 1966, for mathematical analysis and discussion) but may differ in two respects:

1. *Junction Potentials between an Unstirred Layer and a Well-Stirred Bathing Solution.* When the bathing solution on one side of the gallbladder is changed in composition, a junction potential is instantly established between the new bathing solution and an unstirred layer of old bathing solution adhering to the gallbladder surface. As the composition of the unstirred layer gradually equilibrates with the new bathing solution by diffusion, this transient junction potential disappears, and at the same time a new concentration gradient and new steady-state p.d. develop immediately across the gallbladder itself (Fig. 15). Depending upon the relative magnitudes of the junction potential and new steady-state p.d., and upon whether they have the same or opposite orientations, this transient junction potential may range from obvious to undetectable. Fig. 16 illustrates the range of forms encountered in cation biionic potentials. Transient junction potentials associated with dilution potentials and with anion biionic potentials have been illustrated by Diamond (1962, Figs. 3 and 4; 1966, Fig. 5). Examples encountered with biionic potentials of cationic amines are discussed elsewhere (Moreno & Diamond, 1974*b*).

2. *Biionic "Spikes".* When a $K^+:Na^+$ biionic potential is measured in a freshly dissected rabbit gallbladder, the p.d. abruptly rises to a peak of up to 50 mV, then declines with a half time of about 30 sec to a lower steady-state value. A mirror image of this form, although smaller in size, is observed when the mucosal cation is changed from Na^+ back to K^+. Similar behavior but with a lower peak-to-steady-state p.d. ratio is observed for $Rb^+:Na^+$ and $Tl^+:Na^+$ biionic potentials in rabbit gallbladder (Fig. 17). These spikes were noted previously by Diamond and Harrison (1966, Fig. 7) and by Barry and Diamond (1970, Fig. 11), who assumed that they were unstirred-layer effects arising from dissipation of the $X^+:Na^+$ gradient by permeation through the epithelium. These authors therefore calculated P_X/P_{Na} from the p.d. at the height of the spike.

However, four observations suggest that the cause of the spikes is more complex than previously supposed, and that the steady-state value rather than the peak value of the p.d. is the correct one to use for calculating permeability ratios. First, no such transient is observed for $NH_4^+:Na^+$ biionic potentials in rabbit gallbladder, although NH_4^+ and Rb^+ have similar permeabilities as well as free-solution mobilities (Fig. 17). Second, no such transients are observed in frog gallbladder, although absolute cation permeabilities and unstirred-layer thicknesses are similar in frog and

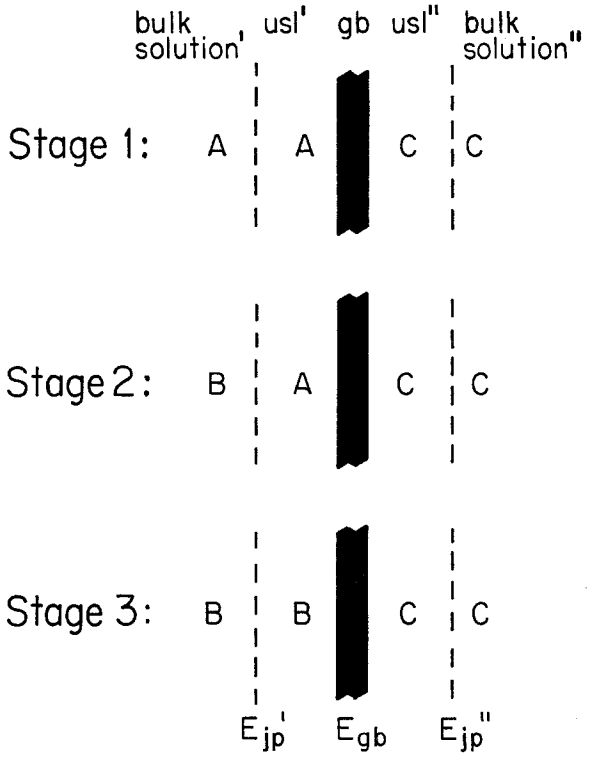

Fig. 15. Contribution of junction potentials to p.d. transients in the gallbladder. The gallbladder itself (*gb*, indicated by black vertical bar) is separated on each side from a well-stirred bathing solution (bulk solution) by an unstirred layer (*usl*) whose limit is indicated by a dashed line. In the steady state (stage 1 or stage 3), when each unstirred layer and the adjacent bulk solution have the same composition, the total p.d. across the system equals the diffusion potential across the gallbladder itself (E_{gb}), determined by its relative permeability characteristics and the compositions of *usl'* and *usl''* (identical to the compositions of bulk solutions ' and '', respectively). Immediately after a change in bulk solution ' (stage 2), a junction potential E'_{jp} transiently appears at the limit of the unstirred layer', in series with E_{gb}, and determined by free-solution mobility ratios and the compositions of *usl'* and bulk solution'. Thus, when bulk solution' is changed in composition from *A* to *B*, the p.d. across the system before zero time (stage 1) is the steady-state value E_{gb} (*A*/*C*), undergoes a transient jump immediately after the solution change (stage 2) to $E'_{jp}(B/A)+E_{gb}(A/C)$, and finally equilibrates (stage 3) to the new steady-state value $E_{gb}(B/C)$. As illustrated in Fig. 16, the resulting transient can assume various forms, depending on the gallbladder permeability ratio, free-solution mobility ratio, composition of solutions *A*, *B* and *C*, and forms of the equations relating E_{jp} and E_{gb} to these parameters

rabbit gallbladders. Third, with repeated application of a K^+:Na^+ or Rb^+:Na^+ biionic gradient, the spike decreases in height and eventually almost disappears, although there is little or no change in the steady-state

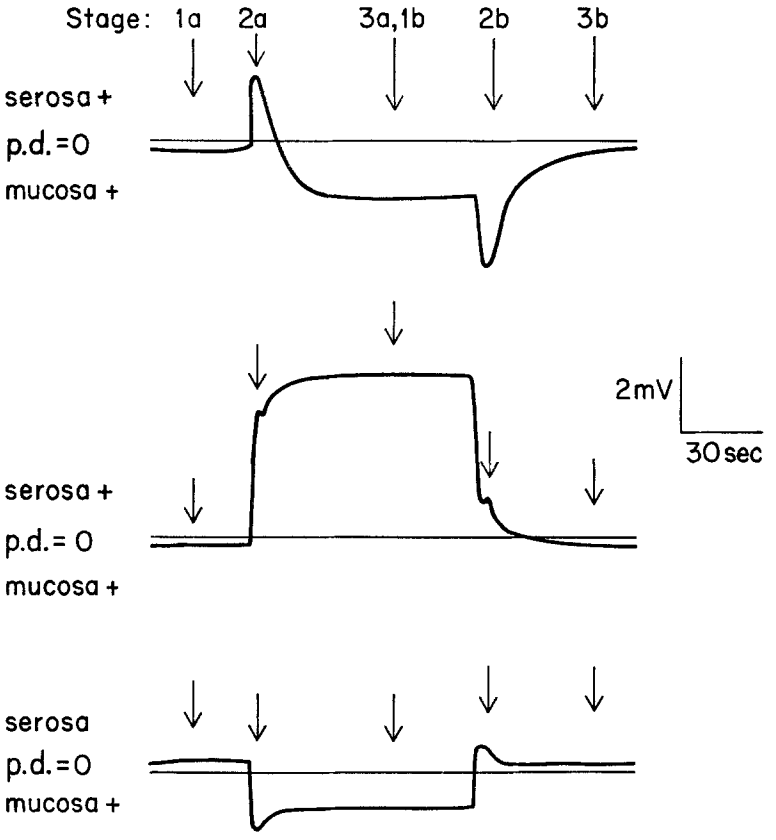

Fig. 16. Types of junction potential transients for cation biionic potentials in gallbladder. Each trace depicts the p.d. change observed when the mucosal solution is initially 150 mM NaCl Ringer's solution (stage 1*a*), is suddenly changed (stage 2*a*) to 150 mM *X*Cl (where *X* is another cation), equilibrates with the mucosal unstirred layer (stage 3*a*=1*b*), is suddenly changed back (stage 2*b*) to 150 mM NaCl, and again equilibrates (stage 3*b*). The serosal solution is 150 mM NaCl Ringer's solution throughout. The origin of the transients is illustrated by Fig. 12. The form illustrated in the upper trace arises when $u_X/u_{Na} \gg 1$, $P_X/P_{Na} \ll 1$ (e.g., rabbit gallbladder, $X=Cs^+$). The form in the middle trace arises when $u_X/u_{Na} > 1$, $P_X/P_{Na} \gg 1$ (e.g., $X=Tl^+$ in frog). The form in the lower trace arises when $u_X/u_{Na} \ll 1$, $P_X/P_{Na} < 1$ (e.g., $X=Li^+$ in rabbit). In cases such as the middle trace, the junction potential transient may be scarcely noticeable except as a notch in the trace

p.d. Finally, the half time elapsed from change of solutions to reach the peak p.d. (<1 sec) is much faster than the half time expected (3 to 4 sec) from the mucosal unstirred-layer thickness as estimated from dilution potentials. This suggests that the spikes arise from a low-resistance ion discriminator in series with the discriminator determining steady-state p.d.'s – e.g., be-

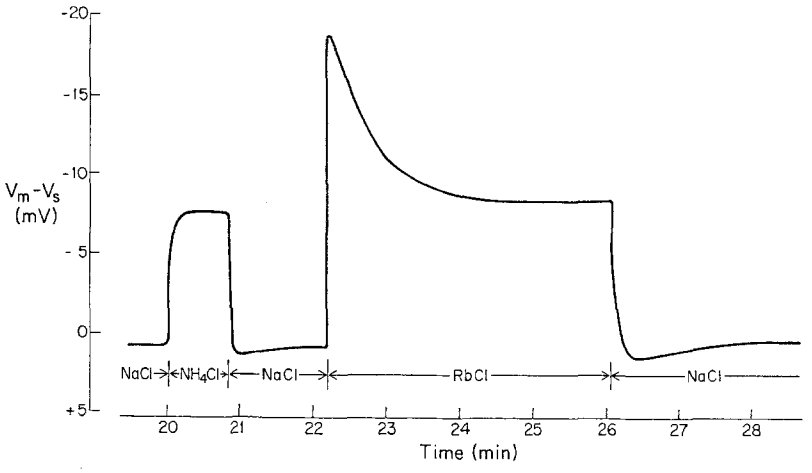

Fig. 17. Biionic potential transients (ordinate: potential of mucosal solution with respect to serosal solution) in a rabbit gallbladder. With both bathing solutions initially 150 mM NaCl Ringer's solutions, the mucosal solution was changed sequentially to 150 mM NH_4Cl, back to 150 mM NaCl, to 150 mM RbCl, and back to 150 mM NaCl. For $Na^+ \rightarrow NH_4^+ \rightarrow Na^+$ changes, the p.d. changes smoothly to a new steady-state value with a halftime of 1 to 2 sec, as expected for diffusional delays in an unstirred layer of 100 μ thickness. For $Na^+ \rightarrow Rb^+ \rightarrow Na^+$ changes, the p.d. initially overshoots the steady-state value, suggesting that a low-resistance ion discriminator is in series with the discriminator determining steady-state p.d.'s

cause sequential elements of a tight junction differ in their selectivity properties, and a low-resistance element with high K^+-Rb^+-Tl^+-Na^+ selectivity lies at the end nearer the mucosal solution. Wiedner and Wright (*personal communication*) have studied the gallbladder spikes in more detail and also concluded that permeability ratios should be calculated from the steady-state p.d.

Reinterpretation of the spikes may resolve three details left unexplained by the studies of Barry *et al.* (1971): that K^+:Na^+ and Rb^+:Na^+ biionic potentials showed more apparent time-dependence than did biionic potentials for other pairs of alkali cations, that this apparent time-dependence did not fully disappear after correction for the shunt (Barry *et al.*, 1971, Table 3), and that there was a significant difference between permeability ratios calculated from diffusion potentials and from biionic potentials for the K^+:Na^+ and Rb^+:Na^+ pairs (Barry *et al.*, 1971, Table 4b). These discrepancies might have been due to use of peak p.d.'s, rather than steady-state values, to extract permeability ratios.

References

Barry, P. H., Diamond, J. M. 1970. Junction potentials, electrode standard potentials, and other problems in interpreting electrical properties of membranes. *J. Membrane Biol.* **3**:93

Barry, P. H., Diamond, J. M. 1971. A theory of ion permeation through membranes with fixed neutral sites. *J. Membrane Biol.* **4**:295

Barry, P. H., Diamond, J. M., Wright, E. M. 1971. The mechanism of cation permeation in rabbit gallbladder. *J. Membrane Biol.* **4**:358

Barry, P. H., Hope, A. B. 1969*a*. Electroosmosis in membranes: Effects of unstirred layers and transport numbers. I. Theory. *Biophys. J.* **9**:700

Barry, P. H., Hope, A. B. 1969*b*. Electroosmosis in membranes: Effects of unstirred layers and transport numbers. II. Experimental. *Biophys. J.* **9**:729

Benzanilla, F., Armstrong, C. M. 1972. Negative conductance caused by entry of sodium and cesium ions into the potassium channels of squib axons. *J. Gen. Physiol.* **60**:588

Berg, H. C., Diamond, J. M., Marfey, P. S. 1965. Erythrocyte membrane: Chemical modification. *Science* **150**:64

Cotton, F. A., Wilkinson, G. 1972. Advanced Inorganic Chemistry. Interscience Publishers, New York

Diamond, J. M. 1962. Mechanism of solute transport by the gall-bladder. *J. Physiol.* **161**:474

Diamond, J. M. 1966. A rapid method for obtaining concentration-voltage relations across membranes. *J. Physiol.* **183**:83

Diamond, J. M., Harrison, S. C. 1966. The effect of fixed charges upon diffusion potentials and streaming potentials. *J. Physiol.* **183**:37

Diamond, J. M., Wright, E. M. 1969. Biological membranes: The physical basis of ion and nonelectrolyte selectivity. *Annu. Rev. Physiol.* **31**:581

Eisenman, G. 1961. On the elementary atomic origin of equilibrium ionic specificity. *In:* Symposium on Membrane Transport and Metabolism. A. Kleinzeller and A. Kotyk, editors. p. 163. Academic Press Inc., New York

Eisenman, G. 1962. Cation selective glass electrodes and their mode of operation. *Biophys. J.*, Part 2. **2**:259

Eisenman, G. 1965*a*. Some elementary factors involved in specific ion permeation. *Proc. XXIII Int. Congr. Physiol. Sci.*, Tokyo, p. 489

Eisenman, G. 1965*b*. The electrochemistry of cation-sensitive glass electrodes. *In:* Advances in Analytical Chemistry and Instrumentation. C. N. Reilley, editor. p. 215. Wiley-Interscience, New York

Eisenman, G., Krasne, S. J. 1973. The ion selectivity of carrier molecules, membranes and enzymes. *In:* MTP International Review of Science, Biochemistry Series. C. F. Fox, editor. Vol. 2. Butterworths, London (*In press*)

Eisenman, G., Szabo, G., Ciani, S., McLaughlin, S. G. A., Krasne, S. J. 1973. Ion binding and ion transport produced by neutral lipid-soluble molecules. *In:* Progress in Surface and Membrane Science. J. F. Danielli, M. D. Rosenberg, D. A. Cadenhead, editors. Vol. 6, p. 139. Academic Press Inc., New York

Frizzell, R. A., Schultz, S. G. 1972. Ionic conductances of extracellular shunt pathway in rabbit ileum. *J. Gen. Physiol.* **59**:318

Frömter, E. 1972. The route of passive ion movement through the epithelium of *Necturus* gallbladder. *J. Membrane Biol.* **8**:259

Frömter, E., Diamond, J. M. 1972. Route of passive ion permeation in epithelia. *Nature, New Biol.* **235**:9

Grell, E., Funck, T., Eggers, F. 1971. Dynamic properties and membrane activity of ion specific antibiotics. *In:* Molecular Mechanisms of Antibiotic Action on Protein Biosynthesis. E. Muñoz, F. García Ferrandiz, E. Vazques, editors. p. 646. Elsevier, Amsterdam

Harned, H. S., Owen, B. B. 1957. The physical chemistry of electrolytic solutions. Reinhold Publishing Corp., New York

Hille, B. 1971. The permeability of the sodium channel to organic cations in myelinated nerve. *J. Gen. Physiol.* **58**:599

Hille, B. 1973. Potassium channels in myelinated nerve: Selective permeability to small cations. *J. Gen. Physiol.* **61**:669

Krasne, S., Eisenman, G. 1973. Molecular basis of ion selectivity. *In:* Membranes—A Series of Advances. G. Eisenman, editor. Vol. 2, Chapter 3, Section V. Marcel Dekker, New York

Ladd, M. F. C. 1968. The radii of spherical ions. *Theoret. Chim. Acta (Berl)* **12**:333

Machen, T. E., Diamond, J. M. 1972. The mechanism of anion permeation in thorium-treated gallbladder. *J. Membrane Biol.* **8**:63

MacInnes, D. A. 1961. The Principles of Electrochemistry. Dover Publications Inc., New York

Moreno, J. H., Diamond, J. M. 1973*a*. Selectivity isotherms for monovalent cations in gall-bladder epithelium. *Fed. Proc.* **32**:217 (Abstr.)

Moreno, J. H., Diamond, J. M. 1973*b*. Selectivity isotherms for permeation of monovalent cations in gall-bladder epithelium. *Nature, New Biol.* **246**:92

Moreno, J. H., Diamond, J. M. 1974*a*. Role of hydrogen bonding in organic cation discrimination by "tight" junctions of gall-bladder epithelium. *Nature (In press)*

Moreno, J. H., Diamond, J. M. 1974*b*. Cation permeation mechanisms and cation selectivity in "tight junctions" of gallbladder epithelium. *In:* Membranes—A Series of Advances. G. Eisenman, editor. Vol. 3. Marcel Dekker, New York (*In press*)

Pauling, L. 1927. *Proc. Roy. Soc. London,* Series A. **114**:181, quoted in Cohen, D. 1962. Specific binding of rubidium in *Chlorella. J. Gen. Physiol.* **45**:959

Pauling, L. 1960. The Nature of the Chemical Bond. Cornell University Press, Ithaca, New York

Pesente, L. 1969. Effetti della concentrazione idrogenionica sulla permeazione di alcuni ioni monovalenti attraverso la pelle di rana. *Soc. Ital. Biol. Sperimentale* **45**:1161

Renkin, E. M. 1954. Filtration, diffusion, and molecular sieving through porous cellulose membranes. *J. Gen. Physiol.* **38**:225

Robinson, R. A., Stokes, R. H. 1970. Electrolyte Solutions. Butterworths, London

Salomon, M. 1970. The thermodynamics of ion solvation in water and propylene carbonate. *J. Phys. Chem.* **74**:2519

Szabo, G., Eisenman, G., Ciani, S. 1969. The effects of the macrotetralide actin antibiotics on the electrical properties of phospholipid bilayer membranes. *J.Membrane Biol.* **1**:346

Teunissen, P. H., Rosenthal, S., Zaaijer, W. H. 1938. Bestimmung der Umladungskonzentration von Trioxystearat und Hexaoxystearat mit Alkali- und Erdalkalichloriden bei verschiedenen pH-Werten. *Rec. Trav. Chim. Pays-Bas* **57**:929

Wedner, H. J., Diamond, J. M. 1969. Contributions of unstirred-layer effects to apparent electrokinetic phenomena in the gall-bladder. *J. Membrane Biol.* **1**:92

Wright, E. M. 1972. Mechanisms of ion transport across the choroid plexus. *J. Physiol. (London)* **226**:545

Wright, E. M., Barry, P. H., Diamond, J. M. 1971. The mechanism of cation permeation in rabbit gallbladder. Conductances, the current-voltage relation, the concentration dependence of anion-cation discrimination, and the calcium competition effect. *J. Membrane Biol.* **4**:331

Wright, E. M., Diamond, J. M. 1968. Effects of pH and polyvalent cations on the selective permeability of gall-bladder epithelium to monovalent ions. *Biochim. Biophys. Acta* **163**:57

Wright, E. M., Diamond, J. M. 1969. An electrical method of measuring nonelectrolyte permeability. *Proc. Roy. Soc.* (*London*), *B.* **172**:203